



CHALMERS
UNIVERSITY OF TECHNOLOGY



Carbon Dioxide Capture Using Phase Changing Solvents

A comparison with state-of-the-art MEA technologies

Master's thesis in Innovative and Sustainable Chemical Engineering

JOHAN ASKMAR
JONATHAN CARBOL

Department of Energy and Environment
CHALMERS UNIVERSITY OF TECHNOLOGY
Gothenburg, Sweden 2017

MASTER'S THESIS 2017

Carbon Dioxide Capture Using Phase Changing Solvents

A comparison with state-of-the-art MEA based technologies

JOHAN ASKMAR
JONATHAN CARBOL



CHALMERS
UNIVERSITY OF TECHNOLOGY

Department of Energy and Environment
Division of Energy Technology
CHALMERS UNIVERSITY OF TECHNOLOGY
Gothenburg, Sweden 2017

Carbon Dioxide Capture Using Phase Changing Solvents
A comparison with state-of-the-art MEA based technologies
Johan Askmar
Jonathan Carbol

© JOHAN ASKMAR & JONATHAN CARBOL, 2017.

Supervisor: Stavros Papadokonstantakis, Department of Energy and Environment
Examiner: Stavros Papadokonstantakis, Department of Energy and Environment

Master's Thesis 2017
Department of Energy and Environment
Division of Energy Technology
Chalmers University of Technology
SE-412 96 Gothenburg
Telephone +46 31 772 1000

Cover: ©Smoke One, Halifax by Owen Byrne through Creative Commons licence.
<https://www.flickr.com/photos/ojbyrne/2167696800>

Typeset in L^AT_EX
Printed by Chalmers Reproservice
Gothenburg, Sweden 2017

Carbon Dioxide Capture Using Phase Changing Solvents
A comparison with state-of-the-art MEA based technologies
JOHAN ASKMAR
JONATHAN CARBOL
Department of Energy and Environment
Chalmers University of Technology

Abstract

In order to combat climate change Carbon Capture and Storage (CCS) has been suggested as an important tool to reduce the emissions of the potent greenhouse gas carbon dioxide (CO_2). CCS can be used for large point source emissions of CO_2 , like power plants using fossil fuels, where it removes CO_2 from the flue gases. This is most commonly done through the use of chemical absorption of CO_2 in an amine solvent called monoethanolamine (MEA). After the absorption the solvent is regenerated and the captured CO_2 is released in a stripping column, a process which is both expensive and energy consuming. The energy used for the regeneration reduces the output from the power plants imposing an energy penalty of up to almost 30%. Reducing the energy requirement in the carbon capture process is crucial in order to make CCS commercially viable, and one possible way to do this is to use so-called phase changing solvents. This new family of molecules are amines that in the presence of water and CO_2 exhibit a triple phase vapour-liquid-liquid equilibrium. The liquid mixture separates into two liquid phases where one has a high CO_2 and amine content while the other phase consists mainly of water. The two liquids can be separated without the addition of energy in a decanter so that only a part of the flow is sent to the stripper. This opens up new possibilities for the design of absorption/desorption flowsheets for solvent based CCS that may reduce the total energy requirement of the process. Creating flowsheets that can be used for future reference and identifying important aspects and challenges of simulating CCS processes with phase-changing solvents is of importance. Apart from this the aim of this project is to achieve a regeneration energy requirement below 2.0 GJ/tonne CO_2 captured and reduce the operating cost by 80% compared to an MEA reference process.

The project consisted of three parts where the first part was a literature study to identify and select solvents that exhibit the desired phase changing properties followed by property estimation of these solvents in Aspen Plus[®]. The estimated properties were also validated using reference values. Secondly, different flowsheets were created identifying different layout possibilities and a sensitivity analysis was performed investigating the impact of the biggest uncertainties in assumptions made as well as differences in operating conditions. The third part was an economic and environmental assessment of the process and a comparison with an MEA reference process.

In a previous study ten potential phase changing solvents, referred to as D1-D10, had been identified. From this list the solvents that were chosen for this project

were (3-[1-(dimethylamino)propan-2-yl]aminopropyl)dimethylamine, called D6, and 2-[2-(methylamino)ethyl]aminoethan-1-ol, called D9, based on their phase equilibrium. Of these two solvents, D9 overall showed the most promising results. A base case flowsheet layout and two different variations were considered, where both variations reduced the energy demand compared to the base case. Flowsheet Layout 1 where the decanter placement was changed from after to before the heat exchangers showed the largest decrease in energy consumption. The best result was thus obtained from D9 using Layout 1 which has an operating cost of 30.10 EUR/tCO₂ captured, a reduction of over 37% compared to the MEA process. The regeneration energy demand for this process was 1.46 GJ/tCO₂ captured, which is well below the target. The three environmental indicators used (Cumulative Energy Demand, Global Warming Potential and ReCiPe) all point to the processes using D9 being more environmentally friendly than MEA. The results for D6 are not as promising as for D9, which is mostly due to the high reboiler duty of the D6 processes. When using flowsheet Layout 1 the reboiler duty is decreased also for D6 bringing all environmental metrics to levels lower than for MEA, although not as low as D9. However the operating cost is still high which is due to the high price of D6 offsetting the benefits of reduced heat demand.

Sammanfattning

Koldioxidinfångning och lagring (CCS) har föreslagits som ett viktigt redskap för att minska utsläppen av växthusgasen koldioxid (CO₂) med syftet att motverka klimatförändringar. CCS kan användas för att avskilja CO₂ från rökgaserna från stora punktsläpp av CO₂, som kraftverk baserade på fossila bränslen. Koldioxidavskiljningen genomförs vanligast genom kemisk absorption av CO₂ i ett lösningsmedel, en amin som kallas monoetanolamin (MEA). Efter absorptionen regenereras lösningsmedlet och den infångade CO₂ frigörs i en stripper, en desorptionskolonn, vilket är en process som är både dyr och energikrävande. Då energi används i regenereringsprocessen minskar den levererade effekten från kraftverken vilket leder till en energibestrafning på upp till 30%. Att minska energibehovet för koldioxidinfångningsprocessen är avgörande för att göra CCS kommersiellt gångbart och ett möjligt sätt att uppnå detta är genom att använda så kallade "phase changing solvents", fasförändrande lösningsmedel. Dessa ämnen är aminer som tillhör en ny familj av molekyler som när de blandas med vatten och koldioxid uppvisar en trippelfas-, gas-vätske-vätskejämvt. Av de två vätskefaserna som bildas har den ena en hög CO₂- och aminhalt medan den andra fasen består till stor del av vatten. De två vätskorna kan separeras utan tillförsel av energi i en dekanter så att endast en del av flödet skickas till strippern. Det faktumet öppnar upp nya möjligheter gällande utformningen av flödesscheman för absorption/desorption i lösningsmedelsbaserad CCS som kan minska det totala energibehovet för processen. Att skapa flödesscheman som kan användas för framtida referens och att identifiera viktiga aspekter och utmaningar i simuleringar av CCS-processer med fasförändrande lösningsmedel är av stor betydelse. Utöver det är målet med det här projektet att uppnå ett energibehov för regenerationen som understiger 2.0 GJ/t infångad CO₂ och att minska driftskostnaden med 80% jämfört med en MEA-baserad referenspro-

cess.

Projektet bestod av tre delar där den första delen var en litteraturstudie för att identifiera och välja ut lösningsmedel som uppvisar de önskade fasförändrande egenskaperna, följt av uppskattning av egenskaperna för dessa lösningsmedel i Aspen Plus®. De estimerade egenskaperna validerades med hjälp av referensvärden. Den andra delen bestod av att skapa olika flödesscheman som identifierar olika möjliga processutformningar och att utföra en känslighetsanalys som undersöker inverkan av de största osäkerheterna i antaganden som gjorts så väl som i skillnader i driftparametrar. Till sist gjordes en ekonomisk- och en miljöutvärdering av processen som jämfördes med en referensprocess baserad på MEA.

I en tidigare studie identifierades tio potentiella fasförändrande lösningsmedel, kallade D1-D10. Från denna lista valdes för projektet (3-[1-(dimetylamino)propan-2-yl]amino-propyl)dimetylamin, kallat D6, och 2-[2-(metylamino)etyl]aminoetan-1-ol, kallat D9, baserat på deras fasjämvikter. Av dessa två uppvisade D9 generellt de mest lovande resultaten. Ett flödesschema som fungerade som ett basfall samt två variationer av detta skapades där båda variationerna resulterade i lägre energiförbrukning jämfört med basfallet. Layout 1, där dekantern placerades innan värmeväxlingen, var den variation av flödesschemat som uppvisade den största minskningen i energiförbrukning. Det bästa resultatet erhöles därför från D9 med Layout 1 vilken har en driftskostnad på 30.10 EUR/t infångad CO₂, en minskning med över 37% jämfört med MEA-processen. Energiförbrukningen för regenereringen i denna process var 1.46 GJ/t infångad CO₂ vilket väl understiger målsättningen. De tre miljöindikatorer som undersöktes (Cumulative Energy Demand, Global Warming Potential och ReCiPe) tyder dessutom alla på att processerna med D9 är mer miljövänliga än MEA. Resultaten för D6 är inte lika lovande som för D9, vilket till största del beror på den höga energiförbrukningen i strippers återkokare i D6-processerna. När Layout 1 användes minskade energiförbrukningen även för D6 vilket reducerade alla miljöindikatorer till nivåer lägre än de för MEA, men inte lika lågt som för D9. Trots detta var driftskostnaden fortfarande hög vilket beror på det höga priset för D6 vilket motverkar fördelarna med reducerad energiförbrukning.

Keywords: Phase Changing, Solvent, Amine, Carbon Dioxide Capture, CO₂, Aspen Plus, Modelling, Process Design, Energy Reduction.

Acknowledgements

The completion of this report would not have been possible without certain individuals and groups. Firstly we would like to thank the Department of Energy and Environment for the opportunity to do our thesis project at their division. Special thanks goes to Gulnara Shavaliyeva for helping us with the prediction for the environmental impacts of the solvents used. Finally we would like to thank Stavros Papadokonstantakis for guiding us through this project and giving us much needed feedback and help.

Johan Askmar & Jonathan Carbol, Gothenburg, May 2017

Contents

Abbreviations	xii
List of Figures	xvi
List of Tables	xix
1 Introduction	1
2 Background	4
2.1 Carbon capture processes	4
2.2 Transportation and storage	5
2.2.1 Transportation	5
2.2.2 Geological storage	6
2.2.3 Ocean storage	6
2.2.4 Mineral storage	7
3 Theory	8
3.1 Post combustion CO ₂ capture	8
3.1.1 Carbon capture with MEA and with ammonia	9
3.1.2 Phase changing solvents	10
3.1.3 Solvent degradation	10
3.2 Property methods	10
4 Methods	12
4.1 Simulation software	12
4.2 Solvent selection and parameter validation	12
4.2.1 Introducing user defined components to Aspen	13
4.2.2 Assessment of phase equilibrium	13
4.2.3 Validation of properties estimated in Aspen	15
4.3 Chemistry	17
4.3.1 Estimation and setup of reaction product properties	17
4.3.2 Estimation of equilibrium constants	19
4.4 Property methods	20
4.5 Columns - Absorber and Stripper	20
4.6 Decanter	21
4.7 Flowsheets	22
4.7.1 Flowsheet layout variations	22

4.7.2	Sensitivity analysis of the base case	25
4.7.3	Calculation of artificial purge stream	27
4.8	Plant size calculations	29
4.9	Economic assessment	30
4.9.1	Operating costs	30
4.9.2	Capital costs	31
4.10	Environmental assessment	31
4.11	Assumptions	32
5	Results and Discussion	34
5.1	Economic assessment	34
5.1.1	Operating Cost	34
5.1.2	Capital Cost	39
5.2	Environmental assessment	40
5.2.1	Cumulative Energy Demand	40
5.2.2	Global warming potential	42
5.2.3	ReCiPe	44
5.2.4	Regeneration Energy Requirement	46
6	Conclusion	47
6.1	Future work	48
	Bibliography	49
A	Equations related to the property methods	I
B	Ternary diagrams for all design molecules tested	V
C	Calculations of VLL equilibrium	VII
D	Setup of units in Aspen Plus	IX
E	Purge calculations	XII
F	Detailed results of the economic and environmental assessments	XIV
F.1	Economic assessment	XIV
F.2	Environmental assessment	XVII
G	Additional graphs and illustrations	XXI
G.1	Environmental assessment	XXI

Abbreviations & Nomenclature

Abbreviations

Am	Amine
AmCOO ⁻	Carbamate ion
AmH ⁺	Protonated amine
AMP	2-Amino-2-methyl-1-propanol
BC	Base case
Btu	British thermal unit
CAS no.	Chemical Abstracts Service registry number
CCS	Carbon Capture and Storage
CED	Cumulative Energy Demand
CH	Hydrocarbons/Fuel
CO	Carbon monoxide
CO ₂	Carbon dioxide
CO ₃ ²⁻	Carbonate
D6	Design molecule number six
D9	Design molecule number nine
DEA	Diethanolamine
DGA	Diglycolamine
DHAQFM	Aqueous heat of formation
DHFORM	Heat of formation
DS	Degree Scenario
ENRTL/ELECNRTL	Electrolyte Non-Random Two-Liquid
EU	European Union
EUR	Euros
FG	Flue Gases
FU	Functional unit
GWP	Global Warming Potential
H ₂ O	Water
H ₃ O ⁺	Hydronium
HCO ₃ ⁻	Bicarbonate
HEX	Heat EXchanger
IEA	International Energy Agency
L#	Layout #
LL	Liquid-Liquid
LLE	Liquid-Liquid Equilibrium

M	Divalent metal eg. magnesium or calcium
MCO ₃	Metal carbonates
MDEA	Methyl diethanolamine
MEA	Monoethanolamine
MgCO ₃	Magnesium carbonate
Mg ₂ SiO ₄	Forsterite
MO	Metal oxides
mol%	Molar percentage
N ₂	Nitrogen
NH ₃	Ammonia
NIST	National Institute of Standards and Technology
O ₂	Oxygen
PDH	Pitzer-Debye-Hückel
PLXANT	Extended Antoine equation
pp	Percentage point
RCP	ReCiPe environmental indicator
RED	Relative Energy Difference
RK	Redlich-Kwong
S#	Scenario #
SiO ₂	Silicon dioxide
UNIFAC	UNIQUAC Functional-group Activity Coefficient
UNIF-DMD	Dortmund modified UNIFAC
UNIF-LL	UNIFAC for liquid-liquid systems
UNIQUAC	Universal Quasichemical
U.S.	United States
US¢	United States cents
USD	United States dollars
VLL	Vapour-Liquid-Liquid
VLLE	Vapour-Liquid-Liquid equilibrium
wt%	Weight percentage

Nomenclature

α	Split fraction
A_ϕ	Debye-Hückel parameter
c_i	Mass concentration of degradation products
C_p	Heat capacity
d	Density
D_s	Dielectric constant of the solvent
D_w	Dielectric constant of water
η	Electrical efficiency
e	Charge of an electron
em	Carbon emission coefficient
F	Feed stream
γ	Activity coefficient
γ^c	Combinatorial activity

γ^r	Residual activity
g^{ex*}	Molar excess Gibbs free energy
$g^{ex*,Born}$	Born contribution to the molar excess Gibbs free energy
$g^{ex*,LR}$	Long range contribution to the molar excess Gibbs free energy
$g^{ex*,PDH}$	PDH contribution to the molar excess Gibbs free energy
$g^{ex*,SR}$	Short range contribution to the molar excess Gibbs free energy
H_v	Heat of vapourisation
I_x	Ionic strength
k_B	Boltzmann constant
L	Lean stream
L	Compound parameter
K	Equilibrium constant
μ	Viscosity
M_i	Molecular weight of component i
$\dot{m}_{CO_2 \text{ captured}}$	Rate of CO ₂ capture
\dot{m}_d	Degradation product formation rate
\dot{m}_j^i	Mass flow rate of component i in stream j
m_{MEA}^{ox}	Rate of oxidative degradation of MEA
ν	Number of occurrence of functional group
N_0	Avogadro's number
ω	Pitzer accentric fractor
ψ	Area fractional component
Ψ	Group interaction parameter
P	Pressure
P	Mass flow rate of purge stream
P_c	Critical pressure
P_{el}	Electrical output
pKa	Negative base-10 logarithm of the acid dissociation constant of a solution
P_{vap}	Vapour pressure
q_i	Contributions from group volume
r_i	Contributions from group surface area
r_k	Radius of the species k
R	Rich stream
R	Ideal gas constant
RED	Relative energy difference
ρ	Closest approach parameter
σ	Surface tension
$Solpar$	Solubility parameter
θ	Molar weighted segment
Θ	Sum of area fraction of group
T	Temperature

T_{bm}	Boiling temperature
T_c	Critical temperature
T_m	Melting temperature
U_{mn}	Energy of interaction between group m and n
V_m	Molar volume
V_c	Critical volume
x	Mole fraction
X	Group mole fraction
Z	Charge of species

List of Figures

1.1	The emission levels which have to be achieved to reach the different temperature scenarios.	1
1.2	The emission level which have to be achieved using carbon capture and storage to limit temperature increase.	2
2.1	Schematics for the different CCS processes.	5
2.2	Different methods for ocean storage of CO ₂	6
3.1	The basic set up of the carbon capture and storage technology.	8
3.2	Molecular structure of the commonly used MEA molecule.	9
4.1	Flowchart for choosing a suitable property method.	14
4.2	A typical VLLE ternary diagram obtained for the D6/water/CO ₂ mixture at 1.01325 bar.	14
4.3	Molecular structure of (3-{[1-(dimethylamino)propan-2-yl]amino} - propyl)dimethylamine, the D6 design molecule.	15
4.4	Molecular structure of 2-{[2-(methylamino)ethyl]amino}ethan-1-ol, the D9 design molecule.	15
4.5	Aqueous heat of formation for protonated amines as a function of the heat of formation of the corresponding molecular amine.	18
4.6	Aqueous heat of formation for carbamate ions as a function of the heat of formation of the corresponding molecular amine.	18
4.7	Equilibrium constants at different temperatures for amines available in Aspen.	19
4.8	Process layout of the base case, where the rich streams are represented in green, the lean streams in blue and the CO ₂ paths in red.	23
4.9	Layout for the Double Matrix stripper setup.	25
4.10	Simple flowsheet showing where material balances for purge calculations were made.	28
5.1	Operating cost per ton CO ₂ captured for different flowsheet layouts compared to MEA reference flowsheet.	35
5.2	Normalised operating cost comparing base case and scenario 1 for D6 and D9.	36
5.3	Normalised operating cost comparing base case, scenario 2 and scenario 3 for D6 and D9.	37

5.4	Normalised operating cost comparing base case, scenario 4 and scenario 5 for D6 and D9.	37
5.5	Normalised operating cost comparing base case, scenario 6, scenario 7 and scenario 8 for D6 and D9.	38
5.6	Capital cost of CO ₂ capture per MW electricity produced by the power plant.	39
5.7	Cumulative energy demand of the base case layouts for D6 and D9 vs MEA scaled to a CO ₂ capture capacity of one tonne per hour.	41
5.8	Cumulative energy demand variations of the layouts for D6 and D9 vs MEA scaled to a CO ₂ capture capacity of one tonne per hour.	41
5.9	Global warming potential efficiency of the base case layouts for D6 and D9 vs MEA.	43
5.10	Global warming potential efficiency of the layouts for D6 and D9 vs MEA.	43
5.11	The penalty on the Global warming potential for all layouts vs MEA scaled to a CO ₂ capture capacity of one tonne per hour.	44
5.12	ReCiPe points of the base case layouts for D6 and D9 vs MEA scaled to a CO ₂ capture capacity of one tonne per hour.	45
5.13	ReCiPe points of the layouts for D6 and D9 vs MEA scaled to a CO ₂ capture capacity of one tonne per hour.	45
B.1	VLLE ternary diagrams estimated by Aspen for the remaining design molecules not chosen for the project.	VI
C.1	The Vapour-Liquid-Liquid diagrams for amine/water/CO ₂ mixture at atmospheric pressure.	VIII
G.1	Sensitivity analysis of the CED for scenario 1.	XXI
G.2	Sensitivity analysis of the CED for scenarios 2 and 3.	XXII
G.3	Sensitivity analysis of the CED for scenarios 4 and 5.	XXII
G.4	Sensitivity analysis of the CED for scenarios 6, 7 and 8.	XXIII
G.5	Sensitivity analysis of the GWP for scenario 1.	XXIII
G.6	Sensitivity analysis of the GWP for scenarios 2 and 3.	XXIV
G.7	Sensitivity analysis of the GWP for scenarios 4 and 5.	XXIV
G.8	Sensitivity analysis of the GWP for scenarios 6, 7 and 8.	XXV
G.9	Sensitivity analysis of the RCP for scenario 1.	XXV
G.10	Sensitivity analysis of the RCP for scenarios 2 and 3.	XXVI
G.11	Sensitivity analysis of the RCP for scenarios 4 and 5.	XXVI
G.12	Sensitivity analysis of the RCP for scenarios 6, 7 and 8.	XXVII

List of Tables

4.1	Physical properties of the solvents D6 and D9 at 40°C.	16
4.2	The original values estimated by Aspen before they were changed to more suitable ones.	16
4.3	Discretisation points in the liquid film.	21
4.4	Key features of the different layout variations.	24
4.5	Key features of the different sensitivity analyses.	26
4.6	Prices of all utilities used in the processes.	30
4.7	The values of the different resources per functional units for each indicator used.	31
5.1	Utility consumption and operating cost for the D6 and D9 base cases and an MEA reference flowsheet.	34
5.2	Ratio between rich and feed stream in the decanter and water content in the rich phase.	38
5.3	The cumulative energy demand of the different solvents and flowsheet layouts in GJ-eq/tCO ₂ captured.	42
5.4	The GWP efficiency of the different solvents and flowsheet layouts.	44
5.5	The ReCiPe points for D6, D9 and MEA layouts scaled to a CO ₂ capture capacity of one tonne per hour.	46
5.6	The regeneration energy requirement in GJ/tCO ₂ of the different flowsheet layouts.	46
F.1	Capital cost estimations of the D6, D9 and MEA flowsheets performed in Aspen given in USD unless specified.	XIV
F.2	Yearly operating cost for the D6 process in EUR.	XV
F.3	Yearly operating cost for the D9 process in EUR.	XVI
F.4	Yearly operating cost for the D9 process in EUR.	XVI
F.5	Yearly cumulative energy demand of the D6 processes in MJ-eq.	XVIII
F.6	Yearly cumulative energy demand of the D9 processes in MJ-eq.	XVIII
F.7	Yearly global warming potential of the D6 processes in kg CO ₂ -eq.	XIX
F.8	Yearly global warming potential of the D9 processes in kg CO ₂ -eq.	XIX
F.9	Yearly ReCiPe indicator points of the D6 processes.	XX
F.10	Yearly ReCiPe indicator points of the D9 processes	XX

1

Introduction

One of the largest problems facing the world today is climate change, to which carbon dioxide (CO₂) emissions is a major contributing factor. A major agreement between nations to combat climate change, the Paris Climate agreement, was recently made and one of the main objectives of it is to limit the increase of the global average temperature to well below 2°C compared to pre-industrial levels[1]. In order to meet this target, significant changes in policies and technology are necessary. The International Energy Agency has researched which emission levels have to be reached in order to limit the global temperature increase to different scenarios, 6°C, 4°C and 2°C. These scenarios have been visualised using data from the IEA in Figure 1.1, where the 6°C scenario (6DS) is an extrapolation of current trends, and 4DS and 2DS are scenarios where the emissions have been reduced through various means.

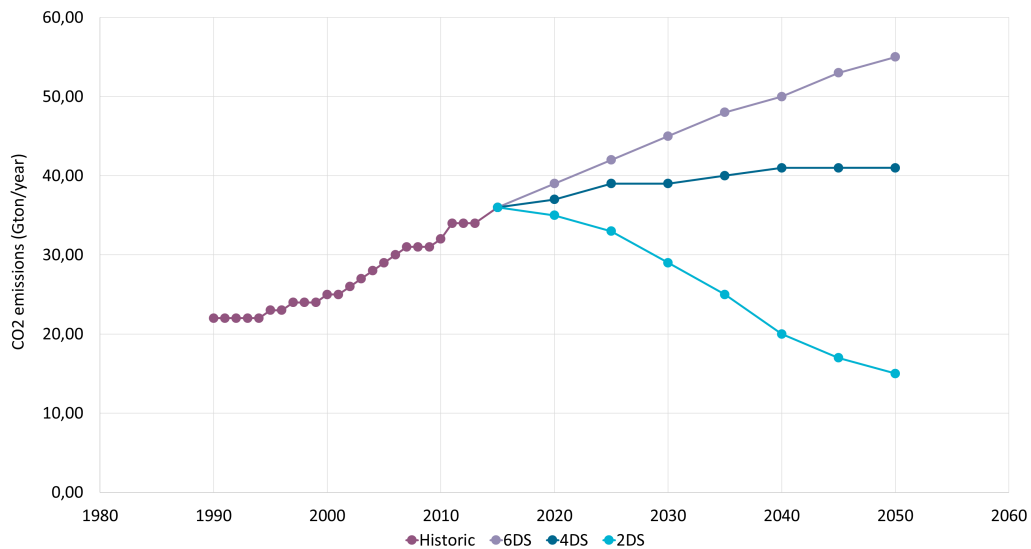


Figure 1.1: The emission levels which have to be achieved to reach the different temperature scenarios.

The 2°C scenario (2DS) predicts trajectories for CO₂ emissions and a pathway for changes in the energy system that has at least 50% chance of limiting the global average temperature increase to 2°C. According to the 2DS, carbon capture and storage (CCS) is a vital part for reaching the targets as it accounts for 12% of the

required reduction in CO₂ emissions[2]. This reduction can be observed in Figure 1.2.

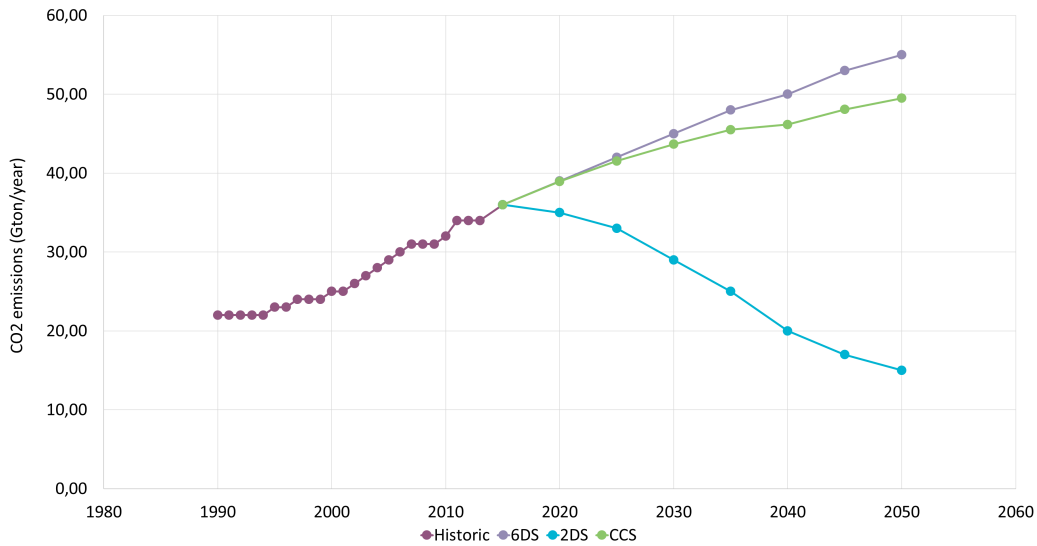


Figure 1.2: The emission level which have to be achieved using carbon capture and storage to limit temperature increase.

One way to perform CCS is to capture CO₂ from flue gases by chemical absorption. The CO₂ is absorbed by a solvent, typically a 30 wt% water solution of monoethanolamine (MEA), in an absorption column. The solvent is regenerated in a stripping column, a process which is both energy consuming and expensive. A typical stripper in an MEA process requires 3.7 GJ/ton CO₂ captured[3]. Since more fuel is needed to compensate for the extra energy used for the regeneration, a cost and energy penalty arises. This penalty varies for different plant types but the energy penalty can range from 14-28%[4]. The lowest penalty occurs for integrated gasification combined cycle plants and the highest for pulverised coal plants with natural gas combined cycle plant in between. The pulverised coal plants have a higher energy penalty than natural gas fired plants due to the larger carbon content in the coal. However, integrated gasification combined cycle plants also use coal but due to the higher CO₂ partial pressure, the more energy efficient physical absorption can be used. As a result of this increased energy demand together with a higher capital cost, the price of the electricity goes up and can even double for the more inefficient plants, eg. the price of electricity of a pulverised coal plant increases from 4.25 to 7.96 US¢/kWh[4]. Consequently, ways of reducing energy consumption and cost are of interest.

As a part of an EU Horizon2020 project, the Division of Energy Technology at Chalmers is investigating a new family of molecules that can be used for solvent based post combustion CO₂ capture. In the presence of water and carbon dioxide these new compounds exhibit triple phase equilibrium (VLL) under the conditions of absorption and/or stripping. As a result of this phase equilibrium, new possibilities for the design of absorption/desorption flowsheets for solvent based CO₂ capture

emerge, specifically with the target to significantly reduce the energy consumption in the solvent regeneration step. This would allow for improvement of both the economic as well as the environmental profile of the process. Some phase changing solvents have been identified in collaboration with other partners in the project, and their properties are currently being estimated. Developing process design alternatives of the absorption/desorption processes based on these phase changing solvents is very important, and so is assessing them from techno-economic and sustainability perspective.

The aims of the simulations are to achieve a regeneration energy requirement below 2.0 GJ/ton of CO₂ captured, whilst reducing operating cost by more than 80%. The simulation will thereafter be compared to a state of the art MEA based CCS technology[5] to determine their economic and environmental competitiveness.

2

Background

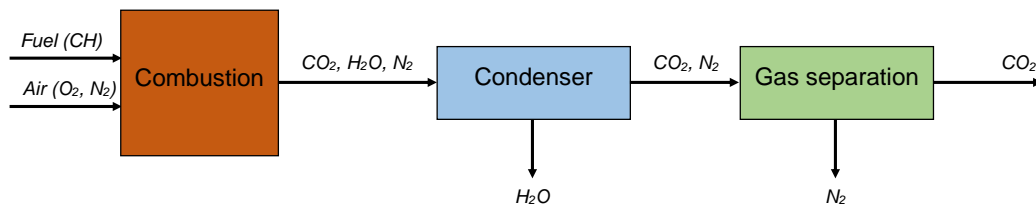
2.1 Carbon capture processes

Carbon capture and storage is the concept of removing CO_2 from effluent gas streams and recovering a high purity stream of CO_2 that can be compressed and stored. There are several different methods for CO_2 capture and they can typically be classified as post combustion capture, oxyfuel combustion or pre combustion capture [4].

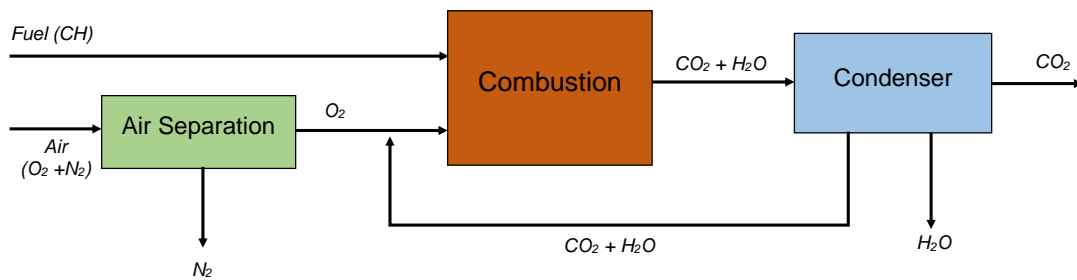
Post combustion carbon capture, Figure 2.1a, is based on removing the CO_2 from the flue gases after the combustion, most commonly through chemical absorption of CO_2 in MEA or some other solvent. After the absorption the CO_2 is then recovered and the solvent regenerated in a stripping process. The main advantage of post combustion processes is that existing processes more easily can be retrofitted to install a post combustion capture technology as it does not require changes in the operation of the combustion process.

Most combustion processes are performed using air as an oxidant and subsequently large amounts of N_2 are present in the flue gases. Separating CO_2 and N_2 is both expensive and energy demanding and as an alternative oxyfuel combustion, Figure 2.1b, can be utilised. Oxyfuel processes are based on another gas separation where oxygen is separated from the nitrogen in air and pure oxygen is then used for the combustion[6]. The flue gases formed consist primarily of CO_2 and water vapour, the latter of which can easily be condensed and removed, resulting in a stream of pure CO_2 .

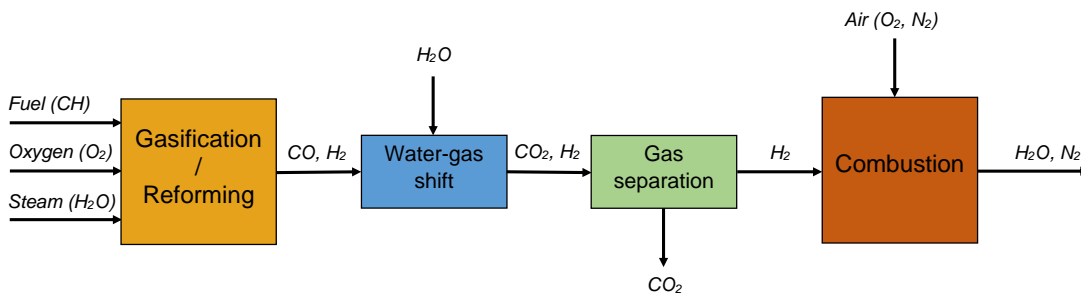
In pre combustion processes, Figure 2.1c, the CO_2 is removed before the final combustion is performed[7]. The first step is partially oxidising the fuel, typically in a gasifier, to form carbon monoxide and hydrogen. The carbon monoxide then reacts with steam in a water-gas shift reaction forming CO_2 and more hydrogen. Hydrogen and CO_2 are then separated and only the remaining hydrogen is burned, with water vapour as the only emission.



(a) Process scheme for the post combustion CCS process.



(b) Process scheme for the oxyfuel CCS process.



(c) Process scheme for the pre combustion CCS process.

Figure 2.1: Schematics for the different CCS processes.

2.2 Transportation and storage

2.2.1 Transportation

Many different approaches have been suggested for the transportation of CO_2 from the capture plant to either storage or further use in other processes. The most prominent and commercially used method is through on-shore pipelines, which is used in multiple locations in the U.S. for enhanced oil recovery. Other transportation methods that have been researched or are used to a lesser extent are motor and water carriers as well as railways[8]. Some of these have advantages over the pipelines, such as utilising already existing infrastructure (roads and railways) or transporting to locations where it is hard or expensive to place pipelines, for example using boats

to transport CO₂ to offshore oil platforms.

2.2.2 Geological storage

Geological storage of CO₂ is a sequestration method that is based on injecting CO₂ into geological formations and storing CO₂ underground. Engineering experience of this technique has been gathered for over 40 years from several enhanced oil recovery projects dating back to the 1970-1980's[9] as well as for CO₂ storage projects like the Sleipner CO₂ storage project which has been operating since 1996[10]. The CO₂ is stored at depths below 800-1000 m where the temperature and pressure causes the CO₂ to reach a supercritical state with liquid-like density[11]. By carefully selecting the site for deep geological storage the CO₂ can be stored for a very long time and it is expected that more than 99 % will be retained for over 1000 years [11]. Geological formations that can be suitable for CO₂ storage include depleted oil and natural gas reservoirs, deep saline aquifers and unminable coal seams [4]. An impermeable layer called caprock prevents CO₂ from being released back into the atmosphere [11].

2.2.3 Ocean storage

Another method for CO₂ storage uses one of the planets largest carbon dioxide sinks; the ocean. The ocean is estimated to have a storage capacity of approximately 1000 Gton CO₂, and multiple ways of storing the CO₂ in the ocean have been suggested.

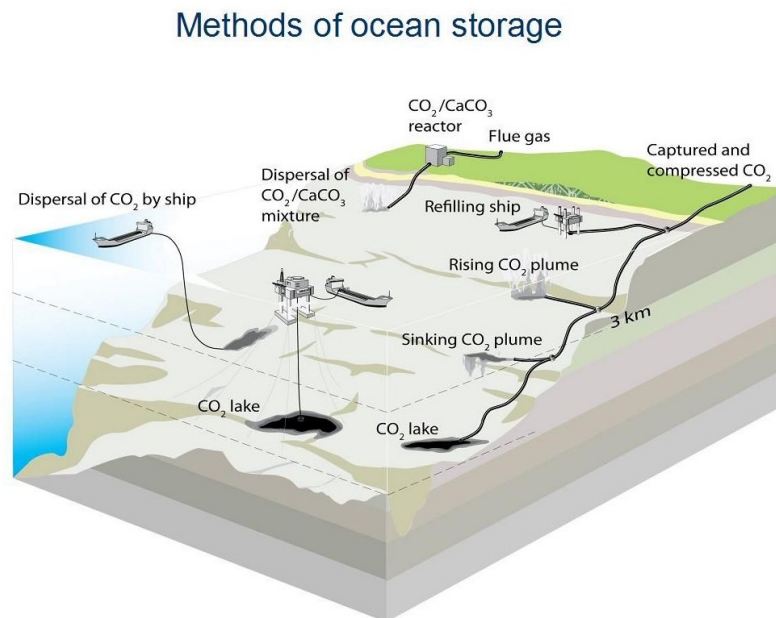


Figure 2.2: Different methods for ocean storage of CO₂.

In Figure 2.2[12], multiple routes for the transport of the CO₂ to the final ocean storage can be seen, as well as some of the different methods for storage. The CO₂ can be pumped deep (below 3km) into the ocean where it, under the high pressure, forms liquid CO₂. This liquid CO₂ sinks to the bottom of the ocean forming CO₂ lakes[12]. It can also be deposited above this depth, where the CO₂ would dissolve into the surrounding water, which is a more cost effective method. These types of storage are still being researched and the best option has yet to be determined.

2.2.4 Mineral storage

The principle behind mineral storage is fixation of CO₂ to form inorganic carbonates in a process called mineral carbonation[13]. CO₂ reacts exothermically with metal oxides according to reaction (2.1), where M represents a divalent metal eg. magnesium or calcium.



The metal oxide-containing material is retrieved from mines and then used in the mineralisation process. Some naturally occurring silicates can be used in the carbonation process including forsterite which reacts with CO₂ according to the following reaction:



The carbonates that are formed are both stable and insoluble, and can be re-used in construction material or disposed of, at for example the original mine site.

3

Theory

3.1 Post combustion CO₂ capture

The capture of CO₂ in a post combustion process is performed by letting the CO₂ absorb into a liquid solvent in an absorption column. The solvent along with the absorbed carbon dioxide is transported to a stripper in which the CO₂ is recovered from the solvent into a vapour stream. The CO₂ is then compressed before being sent to the long term storage. A schematic of the currently used process can be seen in the figure below.

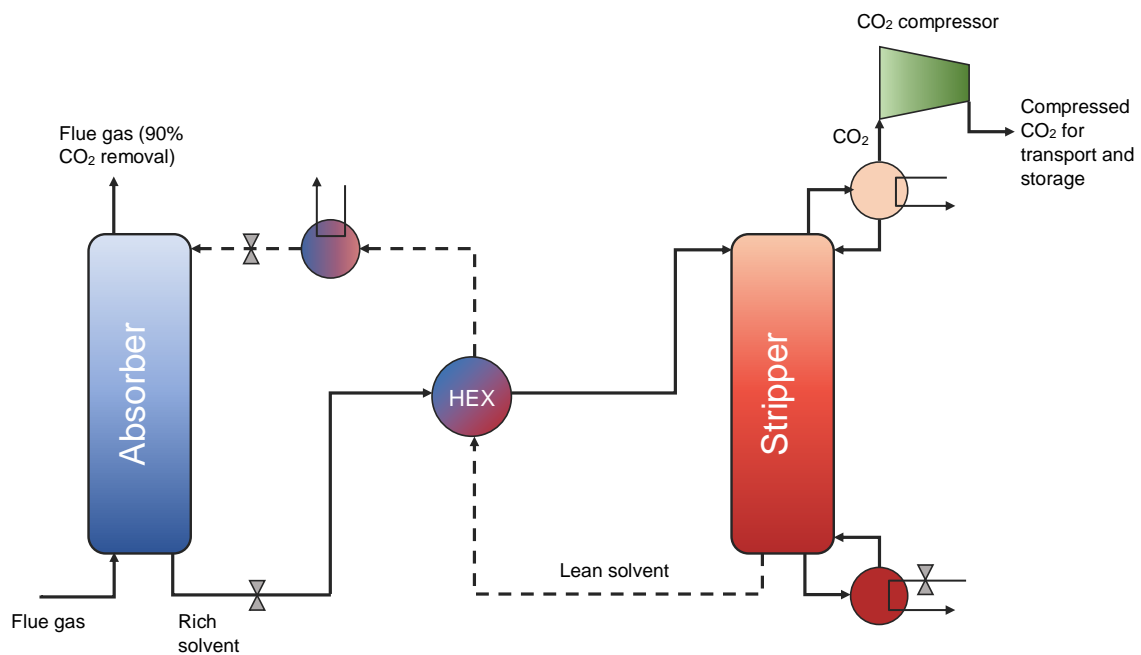


Figure 3.1: The basic set up of the carbon capture and storage technology.

A packed absorption column is usually used to absorb the CO₂ due to the large contact surfaces and efficient mass transfer between the phases. It works with many different solvents such as the most commonly used MEA and NH₃ solvents. The

second important part of the post-combustion CO₂ capture process is the stripper, where the solvent is regenerated. The stripper energy demand of the most commonly used solvents is the main concern with respect to large scale CCS applications.

3.1.1 Carbon capture with MEA and with ammonia

MEA is the most common currently used solvent for CO₂ absorption. It is a primary amine with two CH₂ groups and one OH group as pictured below.



Figure 3.2: Molecular structure of the commonly used MEA molecule.

MEA has been used for acid gas treatment since the first patent of this in 1930 by Roger Bottoms[14]. It only started being used for CO₂ capture in the 1970s not due to global warming but because of the economic benefit of using CO₂ in the enhanced oil recovery process. The most commonly used commercial MEA method for the separation of CO₂ from flue gases is the Fluor Daniel's Econamine FG process, which uses a mixture of 30wt% MEA diluted in water. This reduces the solvent degradation but keeps the loading (calculated using equation (3.1)) of the CO₂ high, resulting in a efficient but energy demanding process for CO₂ separation[15].

$$Loading = \frac{Moles\ of\ all\ CO_2\ carrying\ species}{Moles\ of\ all\ amine\ carrying\ species} \quad (3.1)$$

The process of CO₂ capture using MEA can be seen in Figure 3.1 and includes the standard equipment of an absorber, and intermediary heat exchanger, a stripper and finally a compressor to compress the CO₂ for storage.

The ammonia capture method is quite similar to the standard MEA method, but it is performed at much lower temperatures (0-10 °C) to keep the ammonia from evaporating[16]. The NH₃ process has the additional advantages of NO_x removal[17] and little to no formation of degradation products[18]. This process can however form precipitates in the absorber which can lead to equipment problems but has according to a patent much lower energy demand in the stripping process, than the MEA process[19]. The largest problem of this technology is that the precipitation and slurry formation can lead to plant stop for cleaning. The precipitation occurs due to the formation of ammonium carbonates and the only way to reduce the precipitation is to increase the temperature which might make the process economically challenging[20]. This is still a very new technology and the construction of full scale plants is still limited, thus it is hard to evaluate the results obtained from this technology.

3.1.2 Phase changing solvents

Phase changing solvents are of interest in CCS as they will exhibit a vapour-liquid-liquid equilibrium when mixed with CO₂ and water, at certain temperatures and pressures. This occurs due to the nonideality and immiscibility of the mixture, which allows for a separation of the two liquid phases. This will in the case of CO₂ separation give one CO₂-lean phase consisting mainly of water that is removed and one CO₂ rich stream with a high amine and CO₂ content going to the stripper. This will lead to a reduction in heat demand as less water is heated and evaporated, and thus give the phase changing solvents an advantage over the currently used MEA solvent.

3.1.3 Solvent degradation

Degradation of the amine solvents is a common occurrence. This degradation is usually divided into oxidative and thermal degradation of the amine and can lead to build-up of unwanted degradation products which have to be removed. The oxidative degradation is thought to occur through two reactions, metal complex oxidation and free radical auto-oxidation[21]. Metals have been proven to have both an inhibiting[22] and catalysing effects[23] on the degradation of amines depending on the metal present. These metals are found in the system due to metal corrosion in the equipment, dissolved metal that already exist in the lean amine or from the fly ashes which have carried over into the flue gases[24].

Under conditions of elevated temperature, as occurs in the stripper, rich amine can undergo thermal degradation. The process is also called carbamate polymerisation where amine and CO₂ react to form larger molecules[25]. The reaction pathways and degradation products formed vary depending on the molecular structure of the parent amine although an important reaction that is common for both ethanolamines and ethylenediamines is the formation of five-member rings.

Oxidative degradation occurs to a much larger extent than thermal degradation. For MEA the degradation rates for the two processes are in the order of 0.29-0.73 kg MEA/t CO₂ captured for oxidative degradation[26] and 0.019 kg MEA/t CO₂ captured for thermal degradation[27].

3.2 Property methods

Two different property methods in Aspen are of interest. The first method is the Electrolyte Non-Random Two-Liquid (ELECNRTL) method, which is a property method that is usually used to model CO₂ capture systems. It is a robust and versatile model that can handle solvent mixtures as well as aqueous solvents[28]. This is a necessity when simulating CO₂ using amine solvents.

The ELECNRTL method was first proposed by Chen et al.[29] as a model which

allowed both molecular and ionic solutes in an aqueous system. It calculates the Gibbs free energy of the system using the local composition concept. This concept is based on two assumptions, the first being like ion-repulsion assumption which assumes that the local concentration of cation around cations is zero and vice versa for anions. The second assumption is the concentrations of anions and cations is equal around the solvent.

To calculate the Gibbs free energy, the ELECNRTL model uses sum of the short range force between the different species and the long range electrostatic ion-ion contributions. The model uses the Pitzer-Debye-Hückel equation:

$$\frac{g^{ex*}}{RT} = \frac{g^{ex*,LR}}{RT} + \frac{g^{ex*,SR}}{RT} \quad (3.2)$$

Where g^{ex*} is the molar excess Gibbs free energy, $g^{ex*,LR}$ is the long range contribution to the molar excess Gibbs free energy and $g^{ex*,SR}$ is the short range contribution to the the molar excess Gibbs free energy.

The default ELECNRTL model uses the Redlich-Kwong (RK) equation of state for all vapour phase calculations and the equations used to describe the ELECNRTL method are presented in Appendix A.

The second property model of interest is the UNIQUAC Functional-group Activity Coefficient for Liquid-Liquid systems (UNIF-LL) model. It is used to estimate the activity group contributions of the functional groups for each component in the mixture and it then uses empirical data to calculate the activity coefficients of the whole mixture[30]. These activity coefficients can be used to model the interactions between the molecules and for example determine the liquid-liquid equilibrium of a mixture. This model proposed by Aage Fredenslund *et al.* splits the activity coefficients into two parts, the combinatorial activity and the residual activity contributions:

$$\ln\gamma_i = \ln\gamma_i^c + \ln\gamma_i^r \quad (3.3)$$

Where $\ln\gamma_i^c$ is the combinatorial activity contribution and $\ln\gamma_i^r$ is the residual activity contribution.

The equations for the combinatorial and residual activity contributions are presented in Appendix A.

These two models work well together as the ELECNRTL model is good at handling electrolytes and the chemical reactions. It does however have problems finding the liquid-liquid equilibrium, which the UNIF-LL model excels at. The UNIF-LL model, however, cannot work with ions and can thus not be used as the main model for simulations.

4

Methods

A literature study was performed to find a selection of amine solvents that could be investigated further. Possible solvents had previously been identified by Papadopoulos *et al.*[31] through computer-aided molecular design. The list of candidate solvents were generated from a set of functional groups and then evaluated based on thermodynamic properties, reactivity and sustainability. Ten of the most promising solvents were compiled into series of design molecules, referred to as D1-D10 by Papadopoulos *et al.* These ten design molecules were chosen as the basis for further investigation in this thesis.

4.1 Simulation software

For the simulation part of the project, Aspen Plus[®] v8.8 was used. Aspen Plus[®], which will be referred to as Aspen in this project, is the market leading flowsheeting and simulation tool used for designing, optimising and operating chemical processes. It allows the user to model complex systems using many different process equipment and property methods. It also lets the user add their own molecules and helps estimate any missing properties for the user defined components. This was extremely helpful in this project as it included non-commercial molecules with little to no available data.

4.2 Solvent selection and parameter validation

The design molecule solvents were introduced to Aspen and their properties estimated. Two of the ten molecules were selected after assessment of their respective behaviour at phase equilibrium in a water-CO₂ mixture and the parameters of the estimated properties were validated using reference values of the properties. This process is described in the following section.

4.2.1 Introducing user defined components to Aspen

None of the ten amines D1-D10 existed in available Aspen databases and it was therefore necessary to manually introduce them as user defined components. The components were introduced to Aspen by drawing the molecular structure and using the function *Calculate Bonds* in the *User-Defined Component Wizard* to define the connectivity. When the molecular structure was defined the different properties of the newly introduced components were estimated by the built-in function *Retrieve Parameters* in Aspen. Additional property data was retrieved from the *NIST ThermoData Engine* database for the components that were available.

4.2.2 Assessment of phase equilibrium

As a primary investigation the ability of Aspen to predict the phase splitting, the liquid-liquid equilibrium (LLE) and vapour-liquid-liquid equilibrium (VLLE) of a system containing water, carbon dioxide and amine were studied. When choosing a suitable property method the flowchart in Figures 4.1a and 4.1b was used. Data for representing the reactions involving the solvents e.g. reaction constants were not available. When creating ternary diagrams, like that in Figure 4.2, Aspen was unable to accept any chemistry related information as it could not include the variety of ionic compounds formed in the reactions of the system (see section 4.3). As a consequence the initial screening of the solvents was performed assuming a purely molecular system and ignoring reactions and electrolytes. Since the pressure of the system is moderate and no interaction parameters are available the best property model to represent the system is UNIF-LL, UNIFAC for liquid-liquid systems. UNIFAC methods are based on group contributions from a set of functional groups and several of the design molecules contained a functional group for which UNIF-LL did not have parameters. For these solvents the Dortmund modified UNIFAC method, or UNIF-DMD, had to be used [32], that can also reliably predict various phase-equilibria, including LLE[33].

4. Methods

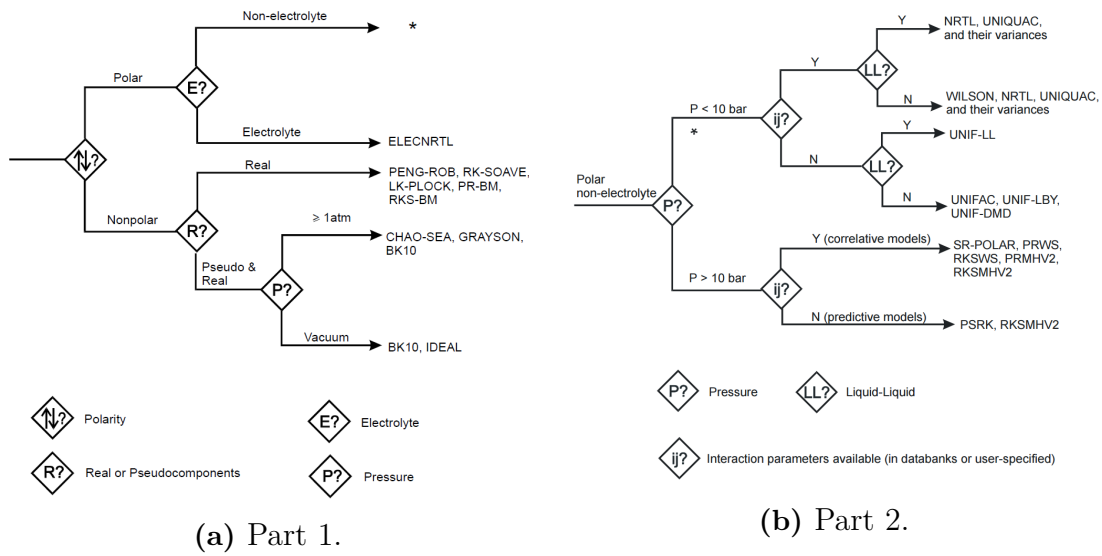


Figure 4.1: Flowchart for choosing a suitable property method.

To examine how Aspen predicted the phase-splitting behaviour of the solvents in the presence of water and carbon dioxide, ternary diagrams were created for each of the solvents of which an example can be seen in Figure 4.2. Outside the phase envelope the system is a single phase mixture while a phase separation occurs and two liquids are formed for mixture compositions inside the envelope. The edges of the tie lines indicate the compositions of the two resulting phases.

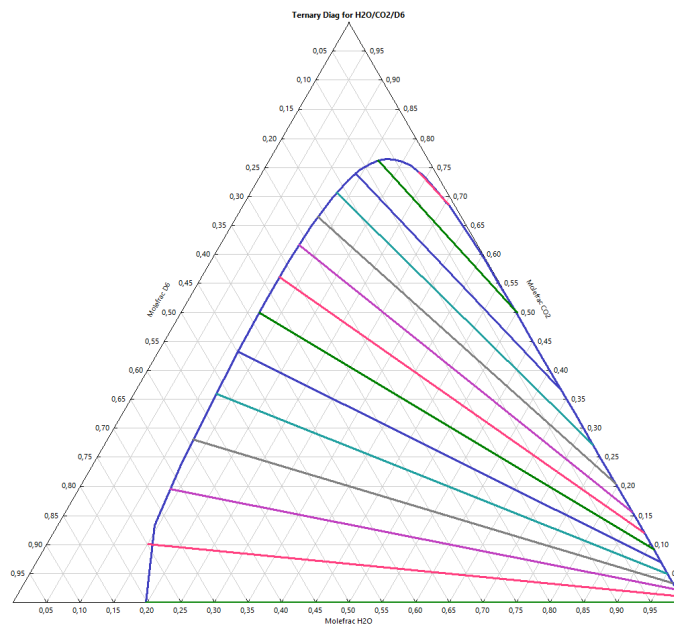


Figure 4.2: A typical VLE ternary diagram obtained for the D6/water/CO₂ mixture at 1.01325 bar.

In order to achieve a significant phase splitting a large envelope is favourable and of

the studied components two amines with promising phase-splitting behaviour were identified: D6 and D9. Their molecular structures are represented in Figures 4.3 and 4.4[31]. The ternary diagrams of the molecules, which showed less promising phase splitting behaviour can be found in Appendix B.

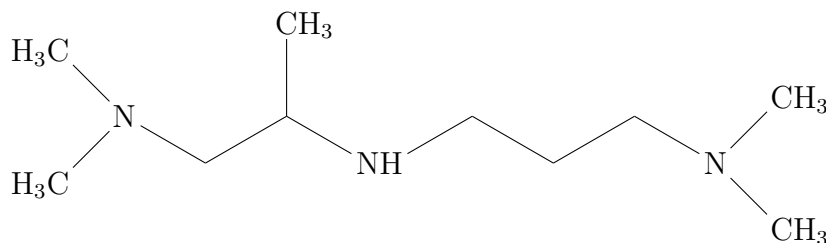


Figure 4.3: Molecular structure of (3-[[1-(dimethylamino)propan-2-yl]amino]propyl)dimethylamine, the D6 design molecule.

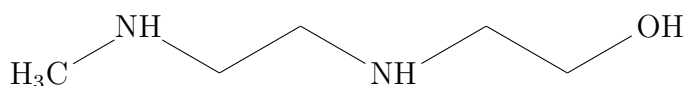


Figure 4.4: Molecular structure of 2-[[2-(methylamino)ethyl]amino]ethan-1-ol, the D9 design molecule.

It is important to note that Aspen only simulates this phase-splitting behaviour due to a physical equilibrium and not an equilibrium based upon the chemistry of the mixture. Thus the way the phase equilibrium is described in these simulations may not be an accurate representation of reality.

4.2.3 Validation of properties estimated in Aspen

Since reference data was not available until later stages of the project, the validation of properties was done only for D6 and D9 after the initial screening of solvents. This means that the ternary diagrams on which the selection was based might have given different results had they been created using validated properties for all design molecules. However when comparing the ternary diagrams for D6 and D9 before and after fitting of properties to the reference values, no significant difference could be seen. It could therefore be reasonable to assume that the ternary diagrams of the rejected molecules would not show large variations either.

The properties calculated from the parameters estimated by Aspen were compared with values that were estimated by the team producing the design molecules. The maximum error that was allowed was 30% and the parameters of any properties that were outside this limit were manually changed or regressed to achieve a better fit. In Table 4.1 the values estimated by Aspen were compared with the predicted values and the error is displayed. The values marked with * are values which have been altered in Aspen in order to obtain an accurate model.

Table 4.1: Physical properties of the solvents D6 and D9 at 40°C.

	D6	D6 Aspen	error [%]	D9	D9 Aspen	error [%]
V_m [cm^3/mol]	223.17	200.7	10.07	122.94	89.6238	27.10
P_{vap} [bar]	4.23e-05	4.23e-05*	2.91e-06	4.43e-06	4.4254e-06*	3.65e-04
σ [dyn/cm]	27.7648	28.8435	3.89	34.2942	34.29*	2.85e-06
C_p [J/molK]	437.86	437.86*	1.06e-07	311.21	311.2643*	0.02
μ [cP]	1.3742	1.3742*	6.82e-05	16.5320	13.4149	18.85
T_m [K]	243.6042	-	-	297.8094	-	-
T_{bm} [K]	497.9785	502.4	0.89	478.7121	495.7	3.55
RED	0.8831	-	-	3.4980	-	-
T_c [K]	671.6639	674	0.35	642.8470	667	3.76
P_c [bar]	17.2232	19.2436	11.73	33.6050	40.0577	19.20
V_c [cm^3/mol]	689.73	696.6	1.44	409.77	391.5	4.46
$Solpar$ [$MPa^{1/2}$]	18.9612	-	-	25.2740	-	-
H_v [kJ/mol]	64.029	64.5843	8.67	72.118	86.0945	19.38
MW [g/mol]	187.3	187.329	0.02	118.18	118.18	0
ω	0.6599	0.6223	5.70	1.1405	1.0189	10.66
pKa	10.08	-	-	9.66	-	-

The original values estimated by Aspen before alterations can be seen in Table 4.2 and are outside 30% of the reference values. The properties which were altered was the vapour pressure and the heat capacity for both D6 and D9, as well as the surface tension for D9 and the viscosity for D6.

Table 4.2: The original values estimated by Aspen before they were changed to more suitable ones.

	D6 Aspen	D9 Aspen
P_{vap} [bar]	4.66e-04	2.42e-05
σ [dyn/cm]	-	52.01
C_p [J/molK]	294.63	209.72
μ [cP]	3.21	-

4.3 Chemistry

To represent the chemistry of a system containing water, carbon dioxide and amine the following four main reactions were used[34]:



Both D6 and D9 contain more than one amine group (that can take part in the aforementioned reactions) but the chemistry was represented with only one site taking part in either of the reactions.

4.3.1 Estimation and setup of reaction product properties

The two ionic forms of the amines, the protonated form (AmH^+) and carbamate form (AmCOO^-), were also introduced to Aspen as user defined components in the same way as their respective molecular form. Although charged groups had been introduced in the molecular structure Aspen did not recognise that AmH^+ and AmCOO^- were ions and therefore did not treat them as such. Since the ions are non-volatile species, the parameters of the extended Antoine equation (PLXANT) had to be manually changed to ensure a negligible vapour pressure of the compounds. Their respective charges were entered as user defined properties under pure component parameters.

In order for Aspen to properly handle the newly introduced ions the aqueous heat of formation (DHAQFM) for the ionic species of the amines was required. Since the amines being used have very little data available this property had to be estimated. By investigating the relationship between the heat of formation (DHFORM) for the molecules and DHAQFM for the different amine ions for amines that already exist in Aspen databases, a linear correlation was found for both AmH^+ and AmCOO^- (Figures 4.5 and 4.6).

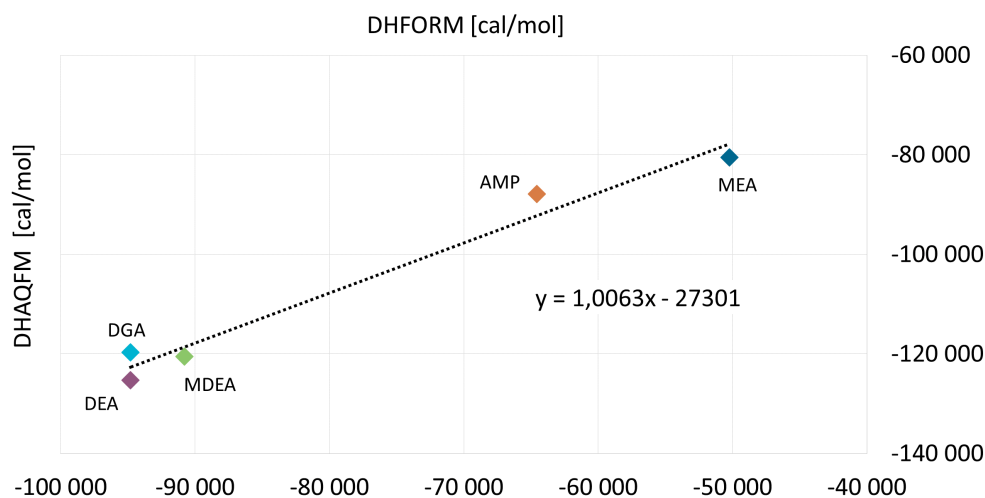


Figure 4.5: Aqueous heat of formation for protonated amines as a function of the heat of formation of the corresponding molecular amine.

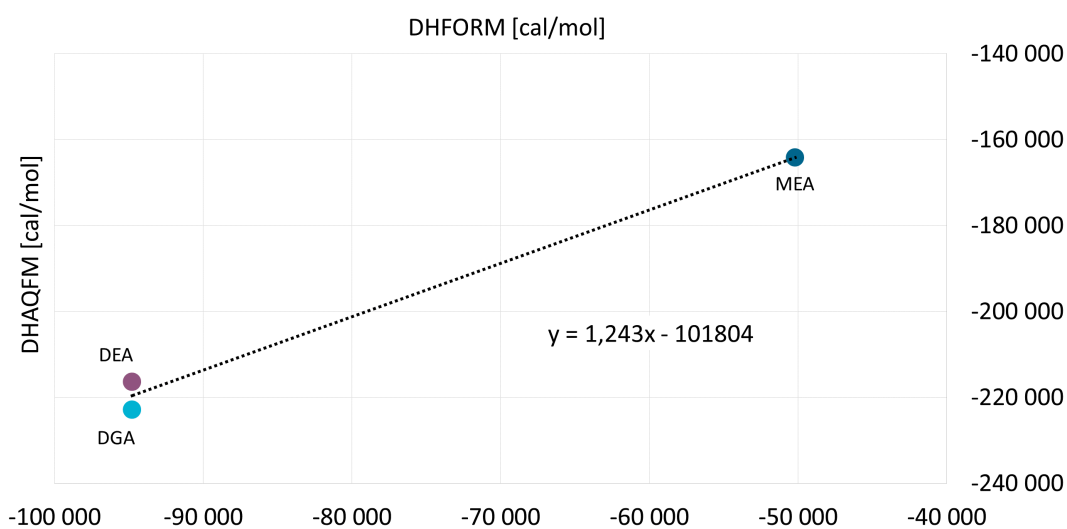


Figure 4.6: Aqueous heat of formation for carbamate ions as a function of the heat of formation of the corresponding molecular amine.

DHAQFM for the studied molecules D6 and D9 were assumed to follow the same linear relation to DHFORM as other amines that already exist in Aspen do. Due to the limited number of data points the linear relation is not very reliable, but still gives an indication of reasonable estimates. DHFORM for the molecular form of the amines were estimated by Aspen and DHAQFM for the ionic forms were thereafter

calculated using the two equations obtained from linear regression of data from the compounds already existing in Aspen databases.

Using the *Elec Wizard*, the other reaction products, H_3O^+ , HCO_3^- and CO_3^{2-} , were added. As Aspen had all necessary data for these molecules, no changes to their properties/parameters were made.

4.3.2 Estimation of equilibrium constants

Values for the equilibrium constants for reaction (4.3) and (4.4) had to be estimated as there are no experimental values available. The temperature dependence of the equilibrium constants for the available amines is shown in Figure 4.7, which shows similarities in the values of the equilibrium constants for the different amines. A smaller $\ln(K)$ causes the equilibria in equations (4.3) & (4.4) to shift to the left, which produces more protonated and carbamate amines respectively. From Figure 4.7 it was possible to get an indication of the order of magnitude of the equilibrium constants for the different reactions.

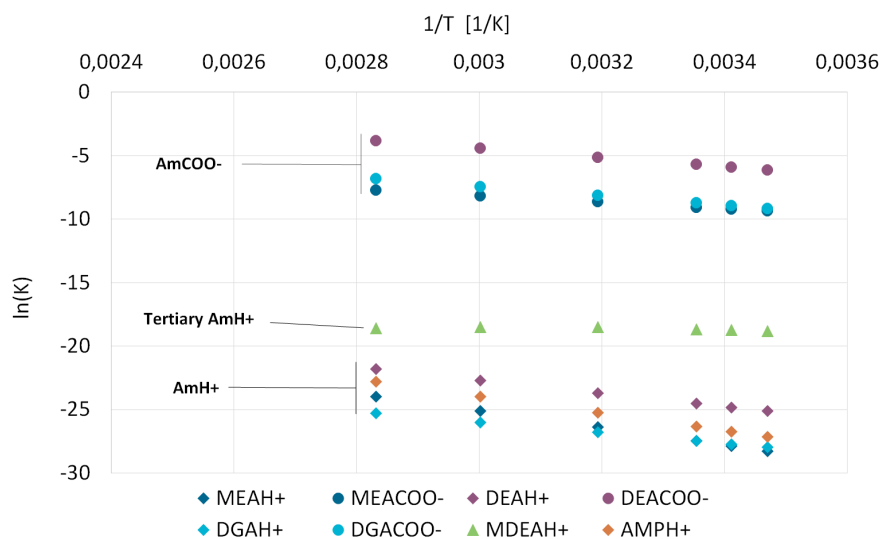


Figure 4.7: Equilibrium constants at different temperatures for amines available in Aspen.

The relative energy difference (RED) number describes a solvent's ability to dissolve a solute. As a consequence the RED number can be used as a qualitative indication of the CO_2 absorption capacity of a solvent. MEA has a high capacity with a RED value of 3.77 and RED for D9 has been estimated to approximately 3.50, which is very similar to MEA. Therefore the chemistry for D9 was simulated using the equilibrium constant values of MEA. D6 has an estimated RED value of 0.88 which is significantly lower than MEA and D9 which indicates that D6 has a much lower capacity for CO_2 absorption. The equilibrium constant values of DEA were instead

chosen to represent D6 as the equilibrium constant of DEA is less favourable for CO₂ absorption compared to MEA.

The equilibrium constants for reactions (4.1) and (4.2), were already supplied within Aspen and were assumed to be accurate.

4.4 Property methods

In order to get accurate results from the simulations, a suitable property method needed to be chosen. The different Aspen property methods were evaluated using the flowchart in Figure 4.1.

Since the simulated system included polar compounds and electrolytes, ELECNRTL and its variations were selected as the most suitable property methods for the simulation of CO₂ capture using phase changing solvents. To ensure that ELECNRTL used the properties fitted according to section 4.2.3, *Property Sets* for the relevant properties were set up in Aspen. The properties were then evaluated in an artificial stream containing only the respective amine at the reference temperature and compared to the values in Table 4.1.

4.5 Columns - Absorber and Stripper

The absorber and stripper in the Aspen simulation were set up as *RadFrac* columns. *RadFrac* columns are rigorous columns in Aspen which excel at various types of chemical calculations including absorbing and stripping. The columns can be modelled using equilibrium or rate-based calculations. Equilibrium calculations assume that the liquid and vapour leaving each stage are in equilibrium, which is not always the case. This is why rate-based calculations was used in the simulations as it corrects the equilibrium assumptions by accounting for heat and mass transfer limitations through stage and Murphree efficiencies, giving more accurate results.

In order to model the absorption and stripping accurately the two-film theory was used and an asymmetric discretisation of the film was used to model the fast absorption/desorption of CO₂ in the liquid film. This asymmetric discretisation was proposed by Kucka *et al.* and uses fewer discretisation points but achieves similarly accurate results to more equidistantly placed point[35] while reducing computational load. Therefore the *Discrxn* method in Aspen was used for the liquid film and since no reactions occur in the gas film, the option *Film* was used. This is the most robust method for film reaction calculations in Aspen and allows the user to decide discretisation points in the film. In order to achieve the asymmetric distribution of the discretisation points the following points were used:

Table 4.3: Discretisation points in the liquid film.

Points	Normalised distance from the vapour/liquid interface
1	0.001
2	0.005
3	0.01
4	0.05
5	0.1
6	0.15
7	0.2
8	0.3

In order to speed up convergence in the flowsheet, the *RadFrac* columns were set up to include absorption/desorption which help the calculations converge. This was further sped up by applying temperature estimates when necessary. The standard material, MellapakTM 250Y from Sulzer was chosen as packing material in the columns to be comparable to the reference MEA process. The MellapakTM 250Y is a packing material which works well for flue gas treatment and usually gives a low pressure drop over the column[36]. To achieve the specified aims of these simulations, design specifications were set up. For the absorber the inlet feed flow was varied in order to achieve 90% absorption of CO₂ from the flue gases. In the stripper, the reboiler duty was varied in order to extract all of the absorbed CO₂ and have a constant amount of CO₂ in circulation. A third design specification was also set up to vary the temperature of the condenser for the vapour from the stripper in order to achieve 98% purity of the CO₂ extracted. A more in depth guide on how the stripper and absorber were set up in Aspen can be found in Appendix D

4.6 Decanter

The ELECNRTL model was in general incapable of estimating the LLE of D6 and D9 since not all required parameters could be retrieved for these solvents. Instead a group contribution method was required for the decanter simulation. UNIF-LL is capable of estimating a phase separation, but is not compatible with the electrolytes present in the system. One possible approach would be to use apparent components to avoid the problem of ions, however this was not possible in the built-in Aspen decanter unit. In order to avoid this issue the phase separation was performed using a separator block which artificially separates components according to user-defined split-fractions and allows using ELECNRTL. Ternary diagrams for a mixture of water, CO₂ and amine were created using the UNIF-LL method and the split fractions could be calculated based on the behaviour of the LLE observed in these diagrams. The calculations relied on material balances of the decanter and compositions obtained from the Aspen simulation as well as from tie lines in the ternary diagrams. The procedure and calculations used are described in appendix C

The bicarbonate and carbonate ions were assumed to separate with the same split fraction as water and the ionic forms of the amines separated with the same split fraction as their respective molecular form.

4.7 Flowsheets

A base case flowsheet was created as a reference to compare different flowsheet variations to. The results of these were also compared to a reference MEA case produced by Gardarsdottir *et al*[5]. In the base case the rich solvent from the absorber was heated through heat exchanging with other process streams. As a consequence of the increased temperature water evaporated and CO₂ desorbed and the resulting vapour phase was removed in an adiabatic flash before the rich stream entered the decanter. CO₂ is desorbed also in the MEA process although not as much as for D6 and D9, but since there is no decanter there is no need to remove this before the stripper. Differences in reaction chemistry and a higher pressure in the heat exchanger of the MEA process could influence the desorption of CO₂. The higher pressure also means that less water evaporates in the MEA process compared to D6 and D9.

In the decanter the split fractions are determined from the ternary diagram based on the LLE between water, solvent and CO₂ at a pressure of 2 bar. In simulations with D6 as solvent the chemistry was modelled using the equilibrium constant values of DEA, while simulations of D9 used values of MEA. Both the absorber and stripper columns were modelled using rate based calculations. The flue gas inlet was specified to have a simplified composition of the MEA reference case. This meant that the flue gases were represented as 11.9 mol% CO₂ with the rest as nitrogen gas (N₂). The inlet entered the absorber at a rate of 339207 m³/hr at 40°C and 1.01325 bar.

4.7.1 Flowsheet layout variations

To evaluate the overall structure of the base case flowsheet, different variations in the flowsheet layout were constructed. The different variations in the layouts are highlighted in Table 4.4.

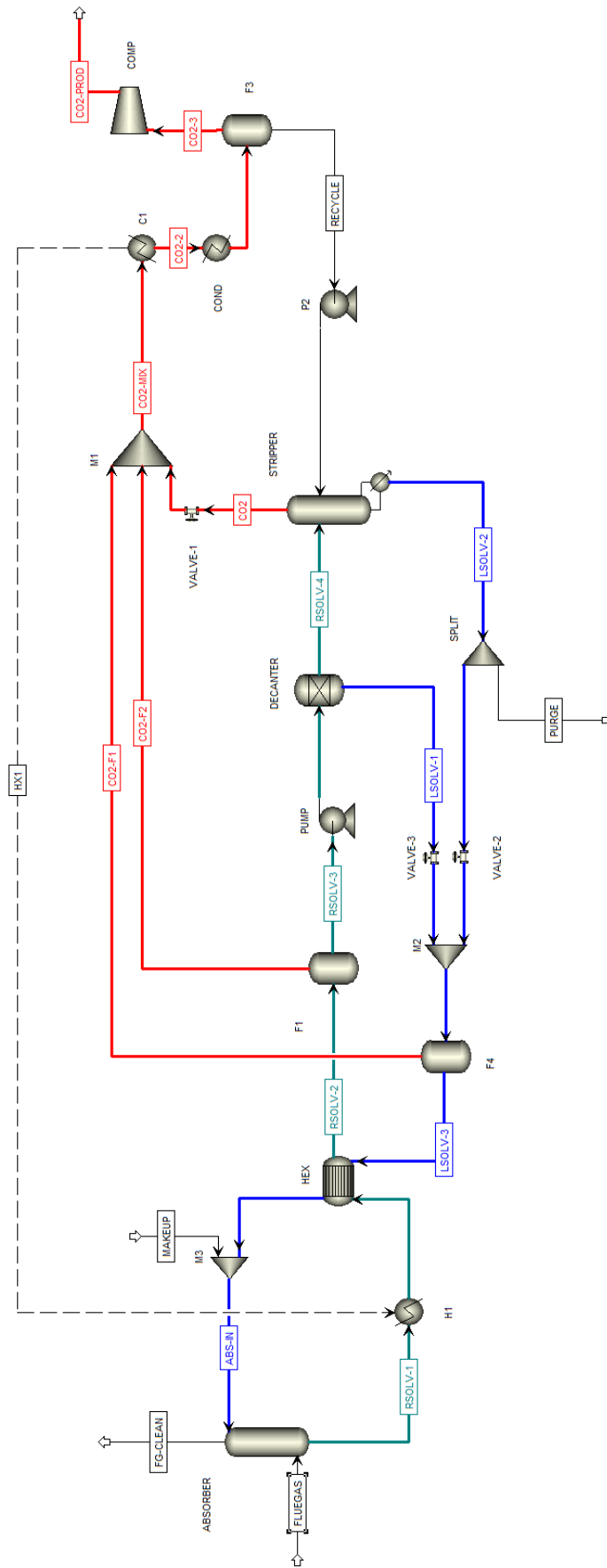


Figure 4.8: Process layout of the base case, where the rich streams are represented in green, the lean streams in blue and the CO₂ paths in red.

Table 4.4: Key features of the different layout variations.

	Sequence	Phase equilibrium	Chemistry D6/D9	Decanter pressure	Rate/Equilibrium based	Comment
Base Case	HX-Flash-Dec	LLE	DEA/MEA	2 bar	Rate	Double Matrix stripper
Layout 1	Dec-HX-Flash	LLE	DEA/MEA	2 bar	Rate	
Layout 2	HX-Flash-Dec	LLE	DEA/MEA	2 bar	Rate	

In Layout 1, the placement of the decanter was changed so that the rich stream exiting the absorber first enters the decanter before heat exchange with other process streams and subsequent flashing to remove the formed vapour phase. In Layout 2 a special stripper configuration was used. After analysing literature a Double Matrix stripper setup was chosen since of the stripper configurations studied it reduced the energy demand the most[37]. This setup uses two strippers operating at different pressures where the rich solvent from the absorber is split between the two strippers. It also uses more advanced heat exchanging so while the stripper duty might be reduced, it will be done on the expense of increased capital cost. The layout of the Double Matrix stripper setup can be seen in Figure 4.9.

4. Methods

known whether the LLE or VLLE ternary diagrams from Aspen best describes the equilibria for the solvents. In scenario 2 the split fractions in the decanter were therefore calculated based on the VLLE ternary diagram. The VLLE is more sensitive to pressure differences and thus scenario 3 investigates this influence of using a lower pressure in the decanter, 1.01325 bar.

Scenarios 4 and 5 examine the effect of how the chemical equilibria are described by increasing and decreasing the equilibrium constants respectively, shifting the equilibrium towards less CO₂ absorption per unit amine in scenario 4 and more CO₂ absorption per unit amine in scenario 5. For D6, the reaction chemistry of MEA was used for the scenario with more absorption whilst the reaction coefficients (K) was reduced by a factor 10 when reducing the absorption in scenario 4. D9 already uses the equilibrium constants of MEA and since it is unlikely that the solvent would be significantly more effective at CO₂ absorption than MEA, a scenario with increased absorption capacity for D9 was not constructed. The scenario with reduced chemistry used a reduced K value of a factor 10 as for D6. The last three scenarios, 6-8, reflect how well separated the two phases out of the decanter are. In scenario 6 & 7, the water content in the rich phase was increased and decreased by 10 percentage points (pp) respectively. In the last scenario, 8, the water content in the lean phase was decreased with 1pp for D6 and 2pp for D9, and thus the split fractions for these scenarios changed.

Table 4.5: Key features of the different sensitivity analyses.

	Phase equilibrium	Chemistry D6/D9	Decanter pressure	Rate/Equilibrium based	Comment
Base Case	LLE	DEA/MEA	2 bar	Rate	
Scenario 1	LLE	DEA/MEA	2 bar	Equilibrium	
Scenario 2	VLLE	DEA/MEA	2 bar	Rate	
Scenario 3	VLLE	DEA/MEA	1.01325 bar	Rate	
Scenario 4	LLE	DEA-/MEA-	2 bar	Rate	Decreased absorption efficiency
Scenario 5	LLE	DEA+/NA	2 bar	Rate	Increased absorption efficiency
Scenario 6-8	LLE	DEA/MEA	2bar	Rate	Altered split fractions

4.7.3 Calculation of artificial purge stream

During the operation of the process the amine solvent will continuously degrade causing an accumulation of degradation products. To avoid a build up of degradation products a slipstream, a part of the lean stream leaving the stripper, is removed and sent to a reclaimer unit where the degradation products are removed and the solvent recovered. The reclaimer is not simulated in this project but instead modelled by removing a fraction of the stripper outlet as an artificial purge stream to account for solvent loss. The purge stream includes both solvent loss due to degradation as well as losses in the reclaimer unit.

The degradation of the solvents D6 and D9 was calculated using the degradation of MEA as a reference. The rate of oxidative degradation of MEA has been estimated to be between 0.29-0.73 kg MEA/tCO₂ captured[26] and D6 and D9 were assumed to degrade at a molar rate equal to that corresponding to 0.5 kg MEA/tCO₂ captured. The mass of solvent degraded through thermal degradation was determined by assuming a ratio between oxidative and thermal degradation of 10:1. The production rate of degradation products is presented in equation (4.7) and was calculated using the stoichiometric relationships in reactions (4.5) and (4.6)[24].



$$\dot{m}_d = \frac{m_{MEA}^{ox}}{M_{MEA}} \left(1.1M_{solvent} + \frac{1}{1.5}M_{O_2} + 0.5M_{CO_2} \right) \dot{m}_{CO_2 \text{ captured}} \quad (4.7)$$

To calculate the solvent losses in the reclaimer unit the ratio between the slipstream and the lean stream leaving the stripper required to maintain a constant concentration of degradation products needed to be determined.

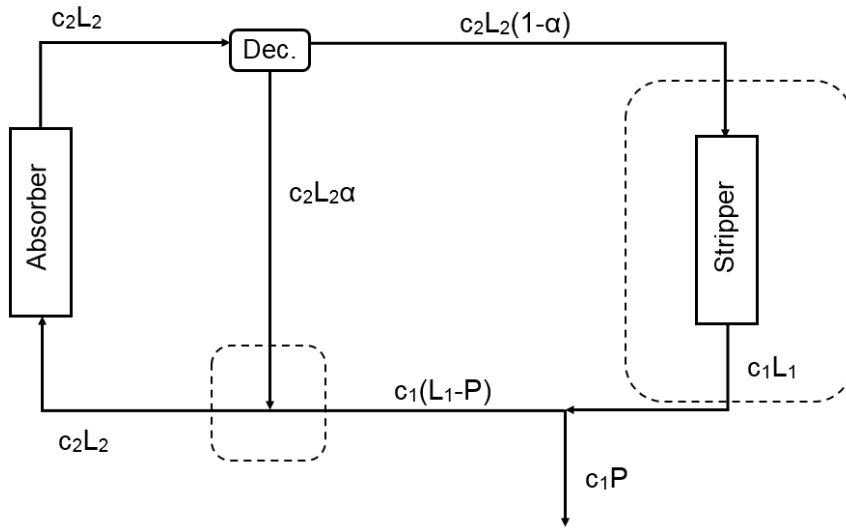


Figure 4.10: Simple flowsheet showing where material balances for purge calculations were made.

Through material balances over the stripper and the mixing point indicated in Figure 4.10 the slipstream ratio could be determined with equation (4.8). L_1 is the mass flow rate in kg/hr of the lean amine stream leaving the stripper and c_1 is the concentration in wt% of degradation products present in the stream. The amount of degradation products is thus c_1L_1 . The amount of degradation products in the stream to the reclaimer unit is c_1P and the amount both entering and exiting the absorber is c_2L_2 . α is the split fraction of the amine species in the decanter unit. It is assumed that the degradation products will behave similarly to the amine and therefore separate with the same split fraction as the amine in the decanter. The rate at which degradation products are formed, \dot{m}_d is measured in kg/hr.

$$\frac{P}{L_1} = \frac{\dot{m}_d}{\dot{m}_d + c_2L_2(1 - \alpha)} \quad (4.8)$$

Of the amine sent to the reclaimer unit in the slipstream it was assumed that 95% would be recovered, resulting in a 5% loss. The total loss of amine due to degradation and inefficiencies in the reclaimer operation was therefore calculated as

$$\dot{m}_{purge} = \dot{m}_d \left(1 + 0.05 \frac{\dot{m}_{L_1}^{amine}}{\dot{m}_d + c_2 L_2 (1 - \alpha)} \right) \quad (4.9)$$

where $\dot{m}_{L_1}^{amine}$ is sum of all amine species in the stream L_1 .

The concentration of recirculating degradation products were kept constant at 1.5% to avoid adverse effects on the energy performance[24] and thus 0.015 was used as a value for c_2 . Values for L_2 and $\dot{m}_{L_1}^{amine}$ were retrieved from the Aspen simulations.

Additional calculations are presented in Appendix E

4.8 Plant size calculations

In order to assess how large cost penalty the CO₂ capture process would mean for a power plant, the type and size of the plant producing flue gases similar to those used in this project had to be estimated. The size of the power plant was calculated using equation 4.10

$$P_{el} = \frac{\dot{m}_{FG}^{CO_2}}{em} \eta \quad (4.10)$$

P_{el} is the electrical output of the plant, $\dot{m}_{FG}^{CO_2}$ is the mass flow rate of CO₂ in the flue gases, em is the carbon emission coefficient for the type of fuel used in the power plant in kg CO₂ per unit thermal energy and η is the electric efficiency of the power plant.

The CO₂ content of the flue gases in the simulations was 11.9% which is close to the content in flue gases from pulverised coal combustion plants of 11%[38]. The flow rate of CO₂ in the flue gases was 1572.31 kmol/hr or 69 197.3631 kg/hr for the D6 and D9 processes and 54 656.28 kg/hr in the MEA process. Using values for carbon emission coefficients for coal of 95.35 kg CO₂/million Btu[39] and assuming an electric efficiency of 38%[40], the size of the power plant was calculated to 80.8 MW for D6 and D9 compared to the 63.8 MW for MEA.

The capital cost of the power plant was assumed to be 3 178 EUR/kW according to 2013 data supplied by the U.S. Energy Information Administration[41] converted into EUR with the exchange rate 0.920469 EUR/USD[42].

4.9 Economic assessment

The economic evaluation of the project was split into operating costs and capital costs evaluations. In order to feasibly compare the carbon capture using phase changing solvents to the currently used carbon capture using MEA the costs were calculated per tonnes of CO₂ captured. Prices and costs that were retrieved in dollars (USD) were converted to euro (EUR) using the exchange rate 0.920469 EUR/USD[42].

4.9.1 Operating costs

The total operating costs is made up of heating cost, electricity cost, cost of process water and cost of amine due to losses. The heating cost is based on any external heating used as well as the heating used in the stripper. The electricity represent the cost of operating pumps for both the MEA case and the D6/D9 cases as well as a compressor used in most of the D6/D9 processes. The reason for using a compressor in the D6/D9 cases is that the CO₂ captured in these cases is at 1.01325 bar whereas the MEA case supplies the captured CO₂ at 2 bar. Process water is lost in the absorber, stripper and the purge. These losses need to be made up for and this is what the cost of process water describes. The cost for loss of amine mostly occur due to degradation of the amine and losses in the reclaiming unit where the degradation products are removed. Finally the total operating cost was compared between the different cases for D6/D9 and MEA as well as the impact of the sensitivity analyses. The operating costs were calculated using prices of utilities presented in Table 4.6 with their costs taken as values for Europe from the Ecoinvent database[43].

Table 4.6: Prices of all utilities used in the processes.

Name	Function unit	Price [EUR/FU]
Heat	1 MJ	0.014
Process water	1 kg	0.00046
Electricity	1 kWh	0.0977
D6	1 tonne	11046
D9	1 tonne	3083
MEA	1 tonne	1767.30

The costs of D6 and D9 were taken from similar molecules, both in molecular weight and in cumulative energy demand. For D6, the price of the molecule with CAS no. 6711-48-4 was used[44] and for D9, the price of the molecule with CAS no. 111-41-1 was chosen[45]. The cost of MEA was taken from literature and was fairly well documented[24].

4.9.2 Capital costs

The capital cost estimates were made using the *Aspen Process Economic Analyzer* in Aspen. In the different D6 and D9 flowsheets the heat exchangers were simulated as separate heaters and coolers with matching duties. The highest cost of the two units in a heater/cooler pair was chosen to represent the cost of a heat exchanger. The capital costs of the designs used in the D6/D9 cases were compared to the more simple layout of the MEA case. The capital cost of the different CCS processes were expressed in relation to the size of the power plant producing the flue gases treated, i.e. the costs were compared in EUR/MW.

4.10 Environmental assessment

The environmental evaluation compares the solvents from different environmental indicators. The indicators that were used are Cumulative Energy Demand (CED), Global Warming Potential (GWP) and ReCiPe (RCP), a point scoring method.

The CED indicator focuses on the energy needed during the life cycle of a product or in this case a process using a specific solvent[46]. It represents energy (MJ-equivalent) needed per functional unit of the resources used. The second indicator, GWP, shows how much greenhouse gases the solvent and utilities produce during their lifetime, converted to CO₂-equivalents[47]. The RCP indicator is the most sophisticated method used in this project, to compare the impact on the environment as it is a summation of different points from eighteen midpoint and three endpoint indicators in order to scale the environmental impact of the process[48]. The environmental indicator values for different resources can be seen in Table 4.7 with the indicator values of heat, process water and electricity taken from the Ecoinvent database using the "at the point of substitution" allocation method for Europe[43]. The indicator values for MEA was taken from literature[24] whilst the values for D6 and D9 were computationally predicted.

Table 4.7: The values of the different resources per functional units for each indicator used.

Name	Functional unit	CED	GWP	RCP
Heat	1 MJ	1.2	0.08	0.008
Process water	1 kg	0.000285	0.0000245	0.000002778
Electricity	1 kWh	11.1	0.48	0.048
D6	1 kg	149.9	5.708	0.9623
D9	1 kg	176.64	6.78	0.4114
MEA	1 kg	97.15	3.455	0.265

4.11 Assumptions

During this project, many assumptions and simplifications have been made in order to give a general idea of the impact of phase changing solvents on CO₂ capture. A list summarising the main assumptions can be found below.

- When comparing the properties estimated by Aspen to the ones predicted by other partners in the project, it was assumed that the predicted values were more accurate than the values estimated by Aspen. It was also assumed that all values estimated or predicted resemble the true values of the molecules used in this project.
- Some values had to be manually entered in Aspen. These values (DHAQFM) for the protonated and carbamated amines had to be regressed from other amines available in Aspen. It was thus assumed that the ions of D6 and D9 follow the same trends represented in Figures 4.5 & 4.6.
- Phase separation of the amine, water and CO₂ was assumed to happen through purely physical means. The chemistry behind this was ignored and thus the results obtained might be inaccurate. It is also possible that other amines than the two selected might produce better results.
- The chemical reactions were represented as equilibrium reactions and no kinetic limitations were imposed.
- The reaction equilibrium for the protonation and carbamation of the amines were assumed to be similar to DEA for D6 and MEA for D9. This might not be accurate but was based upon the RED values for D9 and MEA being similar with D6 having a much lower value which should indicate lower capacity, resulting in the chemistry of DEA being used.
- The molar degradation rate of D6 and D9 was assumed to be the same rate as that of MEA.
- It was assumed that the ratio of oxidative to thermal degradation was 10:1.
- In the reclaimer, it was assumed that beyond the degraded amine, 5% solvent was also lost.
- When calculating the degradation formation for the layout with the double stripper (Layout 2), the concentration of degradation products in the semi-lean and lean streams were assumed to be equal.
- In the decanter, the split fractions of the amine ions were assumed to be the same as their respective amines. This could not be tested as the VLLE/LLE could only be produced for non-electrolyte mixtures.
- In order to simplify the simulations, zero pressure drops over the columns and heat exchangers was assumed.
- To produce capital costs for the base cases and the MEA reference case, it was

assumed that Aspen correctly estimates the capital costs of the plants.

- The environmental indicators values used for D6 and D9 are predictions and thus an assumption is that these predictions are representative for the molecules used.
- As there are no commercial processes for the production of D6 and D9, the price of these is assumed from similar molecules with similar CED and molecular weight.
- Environmental problems related to aerosol formation due to particles in the flue gas or to the waste water treatment of the sludge with the degradation products after the solvent reclaimer were omitted from the study.

5

Results and Discussion

5.1 Economic assessment

Both the operating cost and capital cost are assessed in the results. The different flowsheets for D6 and D9 are compared to a standard MEA flowsheet in a relative costing approach. The electricity required to bring the flue gases into the system as it is similar for all cases.

5.1.1 Operating Cost

One of the main objectives with the project was to reduce the operating cost of the CO₂ capturing process, the main target being the utilities consumption and in particular the heat for solvent regeneration. The operating costs presented in this section are calculated from the cost of different utilities. The utilities that make up the operating cost are heat from low pressure steam required in the stripper reboiler, electricity required for operating pumps and compressors and process water and amine make up due to losses. The cost of cooling water was assumed to be negligible and is therefore not included.

Table 5.1: Utility consumption and operating cost for the D6 and D9 base cases and an MEA reference flowsheet.

	D6 Base Case	D9 Base Case	MEA
Heat [MW]	89.13	30.14	49.97
Electricity [MW]	1.075	0.982	0.028
Process Water [kg/hr]	5892.12	9530.21	2425.21
Amine loss [kg/hr]	334.25	189.47	132.21
Total Cost [MEUR/yr]	66.337	17.629	22.199
CO ₂ captured [t/hr]	62.23	62.26	49.11
Cost per CO ₂ captured [EUR/tCO ₂]	133.21	35.40	56.50

In Table 5.1 the utility consumption and operating costs for the D6 and D9 base cases are compared to an MEA reference flowsheet. The reference flowsheet has

a lower flow rate of flue gases and consequently a lower rate of CO₂ capture. In order to have comparable results the operating cost is also expressed per tonne CO₂ captured. The D9 base case has the lowest operating cost with 35.40 EUR/tCO₂, compared to the MEA reference that cost 56.50 EUR/tCO₂. This reduction in operating cost is mostly due to the much lower reboiler duty in the D9 case. The opposite is true for the D6 base case where a higher heat demand in the reboiler results in a more than doubled operating cost of 133.21 EUR/tCO₂.

Apart from the base case two different flowsheet layouts were created in an effort to improve the process. The operating costs for these layouts are presented and compared to the base case of the respective amine in Figure 5.1. The operating cost of the MEA reference process is also presented.

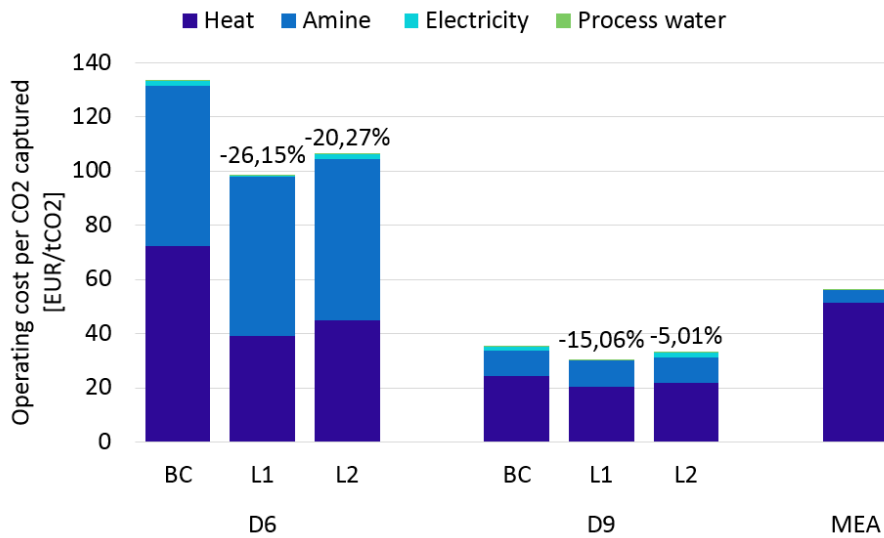


Figure 5.1: Operating cost per ton CO₂ captured for different flowsheet layouts compared to MEA reference flowsheet.

In Figure 5.1, Layout 1 shows the lowest operating cost of the different layouts. In this layout the decanter is placed before the heat exchangers which reduces the flow rate in these. Since the flow being heated is smaller it can reach a higher temperature which means that more CO₂ is released and can be removed in a flash vessel before the flow enters the stripper. This reduces the reboiler duty in the stripper causing a decrease in operating cost. Since the temperature in the decanter is much lower there is a possibility that in a real process the phase separation will be affected more than what was predicted in the simulations, in theory a phase separation might not even occur at such low temperatures. Consequently the phase separation would have to be studied further to determine its temperature dependence before drawing definitive conclusions on the benefit of placing the decanter before the heat exchangers.

Layout 2, the Double Matrix stripper configuration, also reduces the operating cost compared to the base case, although not as much as Layout 1. Apart from the heat requirement making up for amine loss is a major contributor to the total cost. The

high price of D6 (see Table 4.6) is the main reason for the extremely high operating cost compared to D9 and MEA. Reducing degradation and losses in the reclaimer unit could significantly reduce the operating cost of the D6 processes. Figure 5.1 also shows that uncertainties in assumptions regarding degradation rate and price estimations of the amines have a large impact on the end result.

The different scenarios that were created are all based on the base case flowsheet layout and instead vary operating conditions. The different scenarios are compared to the base case where the operating costs per tonne CO₂ captured are normalised to the base case of the respective amine. In Figure 5.2 the impact of operating the absorption and stripping columns with either rate-based or equilibrium calculations is shown.

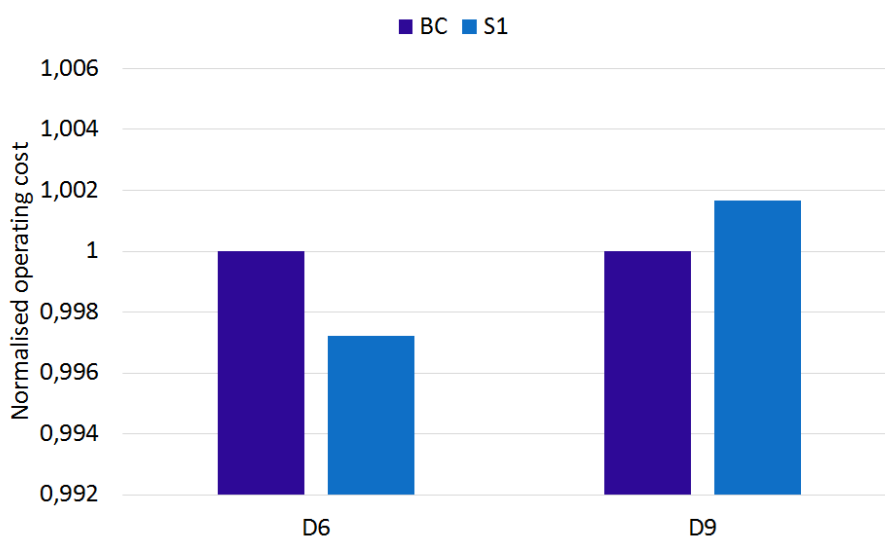


Figure 5.2: Normalised operating cost comparing base case and scenario 1 for D6 and D9.

It can be seen that the effect of equilibrium calculations on the operating cost is very small compared to rate-based calculations, the difference for both D6 and D9 is around 0.2-0.3%. This small difference could be due to the chemistry being represented as equilibrium reactions and thus were assumed to reach equilibrium. In reality it is not certain that the reactions would reach equilibrium due to limitations in kinetics. In this case the error of using equilibrium based instead of rate based calculations might be larger.

One of the large uncertainties in this project is the representation of the phase equilibrium in the decanter. In Figure 5.3 the difference between using ternary diagrams based on LLE (base case) and VLLE (S2 and S3) is shown.

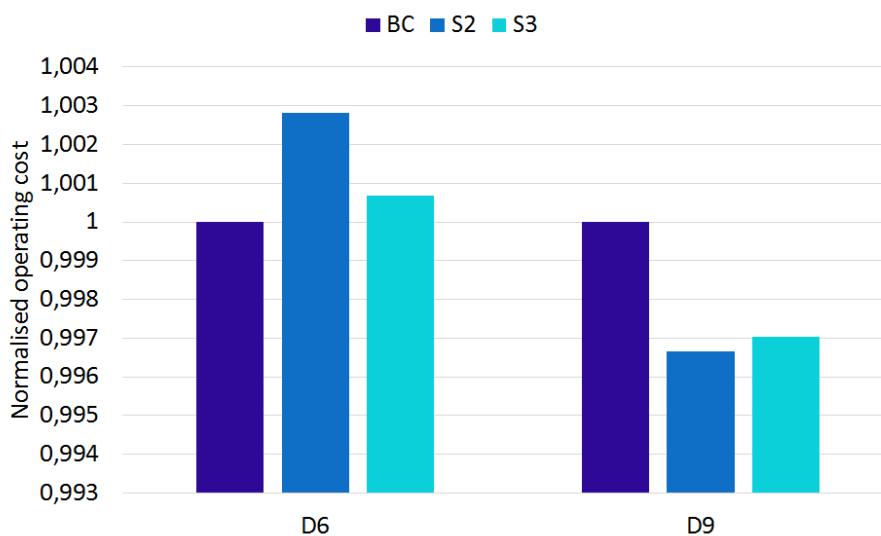


Figure 5.3: Normalised operating cost comparing base case, scenario 2 and scenario 3 for D6 and D9.

This seems to have a limited impact on the operating cost as the largest deviation from the base case is just over 0.3% seen in D6 Scenario 2.

In Scenario 4 and 5 the equilibrium constants for the reactions involving the amines are varied. The effects on the operating cost is presented in Figure 5.4.

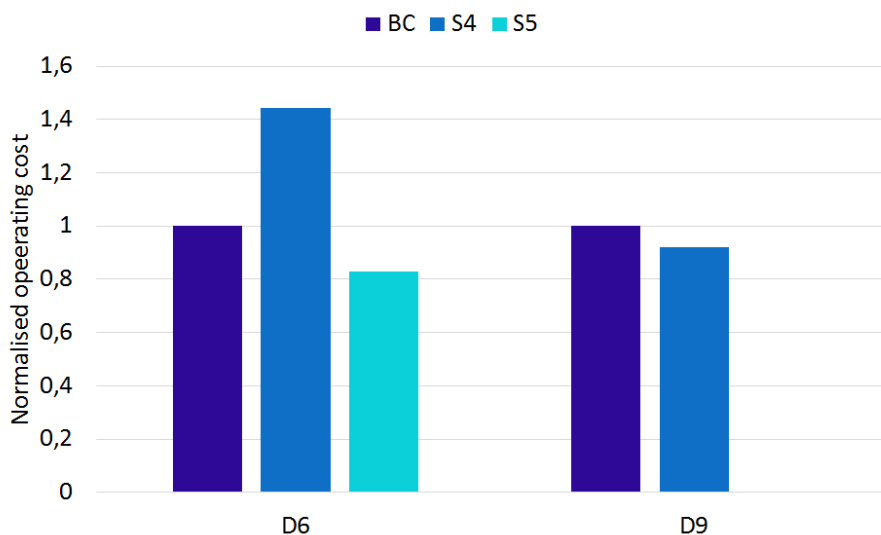


Figure 5.4: Normalised operating cost comparing base case, scenario 4 and scenario 5 for D6 and D9.

From Figure 5.4 it can be seen that the changes made in S4 have opposite effects for D6 and D9. In S4 the chemical equilibrium is shifted so that less of the amine will absorb CO_2 to form a carbamate, and more will remain in the molecular form. For D6, which already has a low absorption capacity, this means that the amount

of amine required to achieve 90% absorption increases, resulting in very large flow rates. As a consequence both solvent losses and pump work, as well as reboiler duty increases resulting in a significant increase of the total operating cost. D9 on the other hand has a reaction chemistry that favours CO₂ absorption. By reducing the capacity the stripping process becomes easier as CO₂ is more readily released from the solution. Even though more solvent is required to achieve the specified CO₂ recovery the reboiler duty decreases compared to the base case resulting in a lower operating cost. For D6 Scenario 5 represents an increased absorption capacity that results in a decrease in operating cost.

Scenarios 6,7 and 8, shown in Figure 5.5 all vary the split fractions in the decanter to investigate the impact of a phase-splitting behaviour that departs from what the ternary diagrams predict.

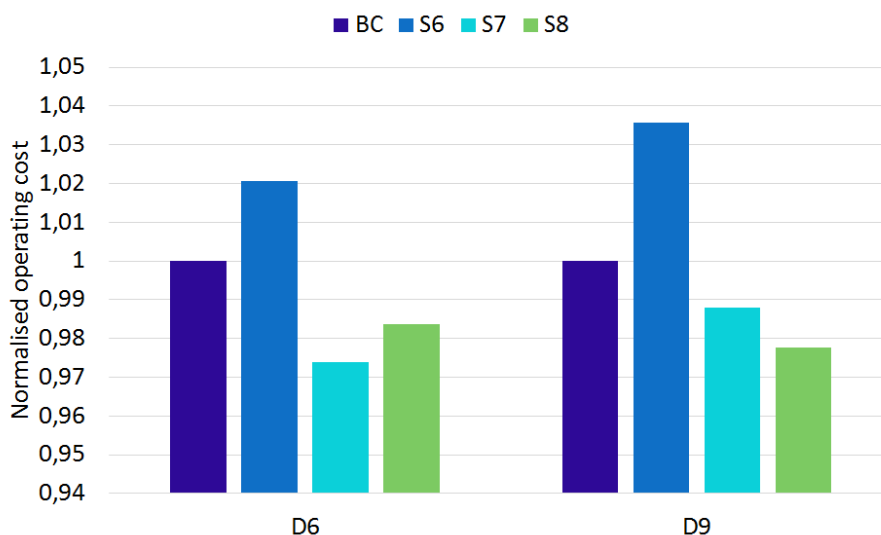


Figure 5.5: Normalised operating cost comparing base case, scenario 6, scenario 7 and scenario 8 for D6 and D9.

Table 5.2: Ratio between rich and feed stream in the decanter and water content in the rich phase.

	D6		D9	
	Split fraction	Water content	Split fraction	Water content
BC	0.126	0.190	0.236	0.588
S6	0.143	0.291	0.337	0.711
S7	0.112	0.091	0.196	0.513
S8	0.112	0.191	0.206	0.612

In Table 5.2 it can be seen that S6 has both the largest fraction of the rich stream entering the stripper and the highest water content for both D6 and D9. This results in the highest operating cost as expected since the larger flow causes a higher energy demand in the stripper. Both S7 and S8 have smaller fractions of the flow entering

the stripper than the base case which also results in lower operating costs. However, in all three scenarios for both D6 and D9 the differences in the result are less than $\pm 4\%$ compared to their respective base case, as can be seen in Figure 5.5.

5.1.2 Capital Cost

In Figure 5.6 the capital cost estimates for the D6 and D9 base cases and the MEA reference case are presented. The capital cost is only a rough estimate meant for comparison between the different flowsheets created and is not meant to represent a full investment cost analysis for the respective capture plants. The cost is expressed per MW of power production capacity of a power plant corresponding to the flue gases being treated. For each process the total cost is separated to show the cost of different units. No systematic optimisation between capital cost and operation cost has been made. For example column sizes are the same for all processes and solvents and could be optimised to each process in order to reduce the capital cost.

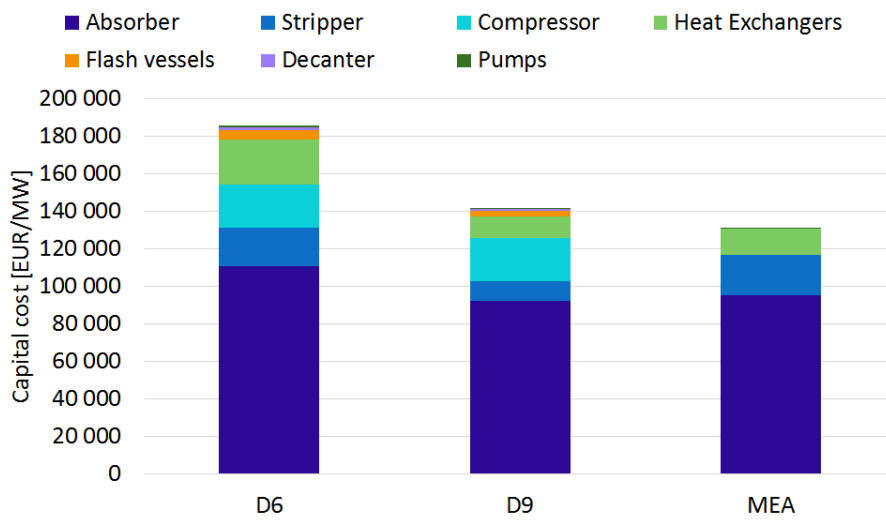


Figure 5.6: Capital cost of CO₂ capture per MW electricity produced by the power plant.

One significant difference between the MEA reference case and the base case of D6 and D9 is that the MEA process recovers CO₂ at 2 bar directly from the stripper and therefore requires no compressor. In reality the captured CO₂ would be delivered at a pressure higher than 2 bar which means that also the MEA process would require a compressor and the difference between the capital cost different processes would be reduced. The compressor cost for D6 and D9 could be reduced by altering the flowsheets to recover the CO₂ from the stripper separately and only use a compressor for the CO₂ from the flash vessels, or by using a multistage compressor if a higher pressure was required. This could be done at the expense of increasing the cost for flash vessels and coolers, since two different CO₂ streams would now require

condensation and removal of water vapour increasing the required number of units. These costs are however small compared to the cost of the compressor it could still reduce the overall capital cost.

The characteristics of the stripper columns are similar for all cases and the differences in stripper capital cost between the processes can therefore be correlated to the size of the reboiler duties in Table 5.1. D6 has the highest heat demand and thus also the highest stripper capital cost and vice versa for D9.

The cost for pumps and for the decanter in D6 and D9 processes are almost negligible while the absorber stands for a majority of the capital cost for all three processes that have been evaluated. Alternative absorber configurations that can achieve the required CO₂ recovery with lower capital cost is therefore something that is worth considering in order to reduce the total capital cost for the CO₂ capture unit.

It is not only important that the operating cost of the CO₂ capture is low, the investment needed for the capital cost must also be of reasonable size. The cost penalty of installing a CO₂ capture unit is 5.85% for D6, 4.46% for D9 and 4.13% for MEA when compared to the 3 178 000 EUR/MW capital cost of the power plant. This means that the total capital cost of building a pulverised coal fired power plant is not significantly increased by installing the CO₂ capture unit.

5.2 Environmental assessment

Other than evaluating the economic efficiency of the CO₂ capture using phase changing solvent, it is also important to see how environmentally friendly the process is. Again the results have been compared to the similar MEA case. In order to do this comparison the utility consumption of heat, electricity, water usage and amine need have been multiplied by the factors shown in Table 4.7 for the respective indicator method used. The results obtained were then scaled to a one tonne per hour capture rate of CO₂, in order to make an easy comparison.

The different sensitivity scenarios have not been as thoroughly evaluated as they showed very similar trends to what the operating cost described. The graphs of the different sensitivity analyses can be found in appendix G. Most sensitivity scenarios had little effect on the environmental impact of the solvents, and the ones that did, the increased or decreased absorption efficiencies, followed the same trend as the operating cost.

5.2.1 Cumulative Energy Demand

One of the main objectives of this project, was to reduce the regeneration energy requirement in the stripper. This accounts for a large part of the cumulative energy demand seen in Figure 5.7.

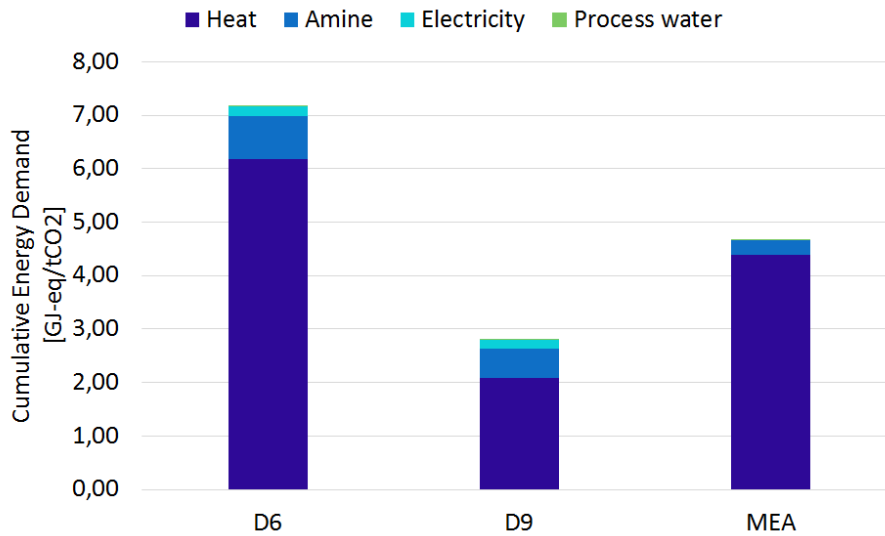


Figure 5.7: Cumulative energy demand of the base case layouts for D6 and D9 vs MEA scaled to a CO₂ capture capacity of one tonne per hour.

When comparing the CED in GJ-eq/tCO₂ captured you can see that for the base cases of D6 and D9 there is a large difference compared to the MEA reference case. The MEA reference case has a CED of approximately 4.66 GJ-eq/tCO₂ captured, whilst D6 and D9 have 7.17 and 2.80 GJ-eq/tCO₂ respectively. This difference mainly arises due to D6 having a larger reboiler duty in the stripper than MEA and D9 having a smaller reboiler duty. The cumulative energy demand however decreases when the layouts of the flowsheets are changed, and this can be observed in Figure 5.8, where BC stands for base case and L1 and L2 stand for Layout 1 and Layout 2 respectively.

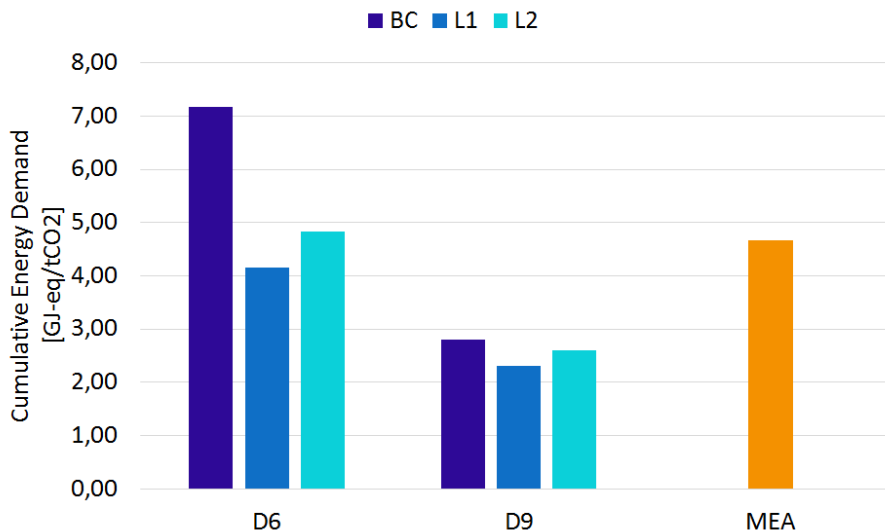


Figure 5.8: Cumulative energy demand variations of the layouts for D6 and D9 vs MEA scaled to a CO₂ capture capacity of one tonne per hour.

Changing to Layout 1 decreases the heat and electricity demand as well as reduces the amount of process water needed in the makeup. This along with an almost constant amine loss reduces the CED by a significant amount for both D6 and D9. The second layout, Layout 2, reduces only the heat demand leaving the other values similar to the base case. This does lead to a smaller but still significant reduction in CED compared to the base case. The exact values of the layouts can be seen in Table 5.3 with more detailed tables over the different contribution found in Tables F.5 and F.6 in appendix B.

Table 5.3: The cumulative energy demand of the different solvents and flowsheet layouts in GJ-eq/tCO₂ captured.

	D6 [GJ-eq/tCO ₂]	D9 [GJ-eq/tCO ₂]	MEA [GJ-eq/tCO ₂]
Base case	7.17	2.80	4.66
Layout 1	4.16	2.30	
Layout 2	4.84	2.59	

From an energy point of view, D6 would be better than MEA when using Layout 1 and almost as good when using Layout 2. It would however be much worse than MEA when capturing CO₂ using the base case layout. Design molecule D9 would however always be better than MEA regardless of which flowsheet layout used when only the CED is taken into account.

5.2.2 Global warming potential

The second indicator that was compared was the global warming potential of the capture process using the different solvents. The efficiency of the capture can be seen in Figures 5.9 & 5.10, where a larger value represents a more efficient CO₂ capture. The axis is defined as the net capture rate scaled by the actual plant capture rate of CO₂ in the process. So a value close to unity describes a solvent which captures the CO₂ without needing a lot of energy or producing a lot of other CO₂ emissions.

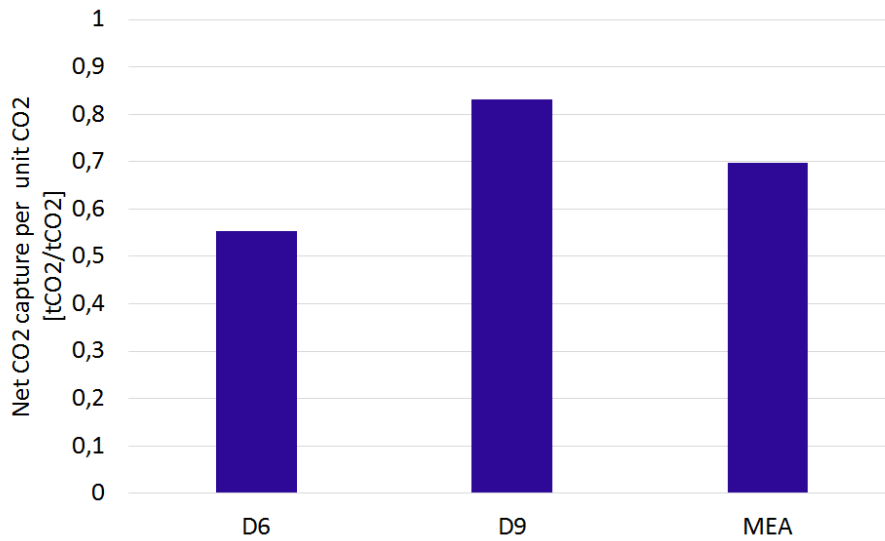


Figure 5.9: Global warming potential efficiency of the base case layouts for D6 and D9 vs MEA.

The most efficient capture when comparing the base cases of D6 and D9 to MEA is D9. As with the cumulative energy demand, this is due to the reduced reboiler duty in the stripper compared to D6 and the MEA case. The trend of the GWP for the different layouts follow the trends of both the operating cost and the CED as shown in Figure 5.10 below.

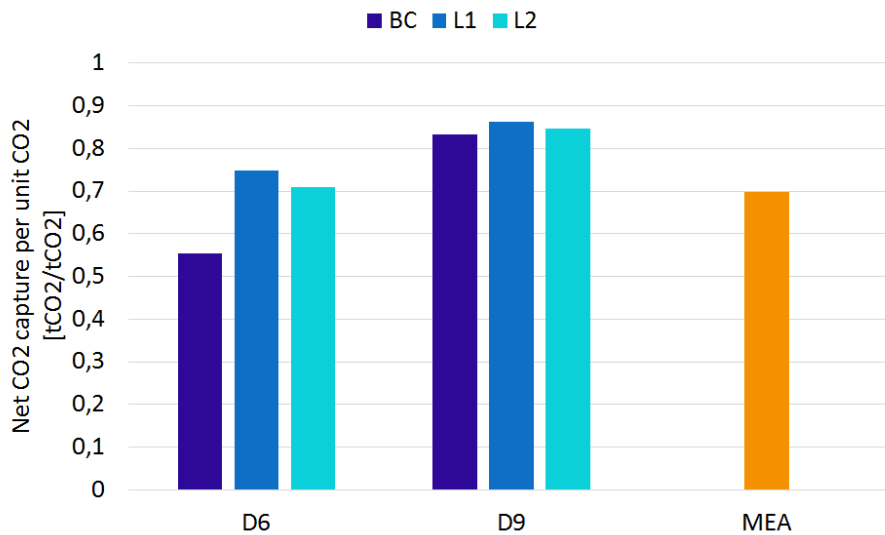


Figure 5.10: Global warming potential efficiency of the layouts for D6 and D9 vs MEA.

When comparing the different layout changes made to the MEA case, it can be seen that both the D6 layout changes become better than the reference MEA case, whilst all D9 layouts are an improvement over MEA. The values describing the efficiency of the global warming potential of D6, D9, MEA, and their layouts can be seen in

Table 5.4 with more detailed tables over the different contribution found in Tables F.7 and F.8 in appendix B.

Table 5.4: The GWP efficiency of the different solvents and flowsheet layouts.

	GWP D6	GWP D9	GWP MEA
Base case	0.555	0.832	0.697
Layout 1	0.747	0.862	
Layout 2	0.710	0.847	

Instead of showing the efficiency of the CO₂ capture process, it might be interesting to view the penalty in global warming potential when using different solvents. This penalty can be described as the emissions in tonnes of CO₂ needed to capture 1 tonne of CO₂ in the capture plant. The penalties can be seen in Figure 5.11, with the D6 base case having the largest penalty of $\approx 44.5\%$ and D9 Layout 1 having the smallest penalty of $\approx 13.8\%$.

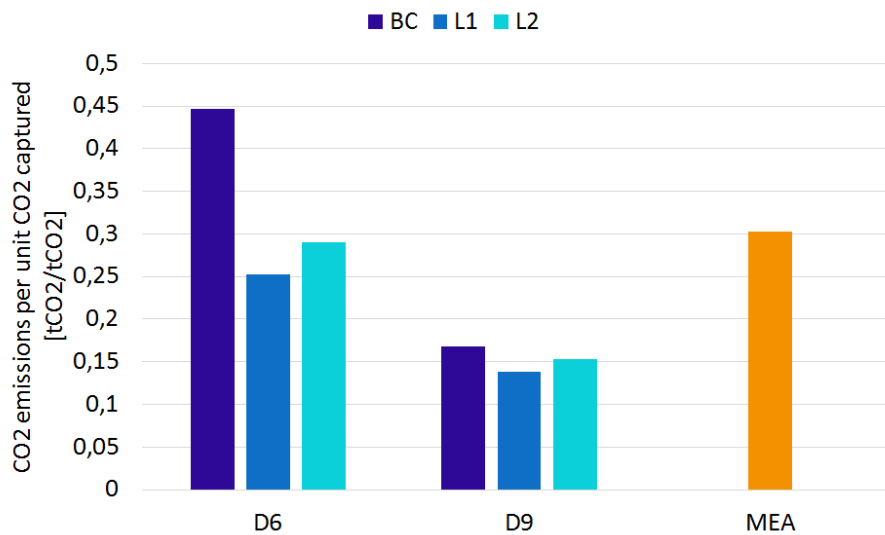


Figure 5.11: The penalty on the Global warming potential for all layouts vs MEA scaled to a CO₂ capture capacity of one tonne per hour.

5.2.3 ReCiPe

The third and final indicator used was the ReCiPe indicator which in Figures 5.12 and 5.13, give points scaled to one tonne of CO₂ captured per hour. When using the ReCiPe indicator, it is important to note that a lower score represents a smaller environmental impact.

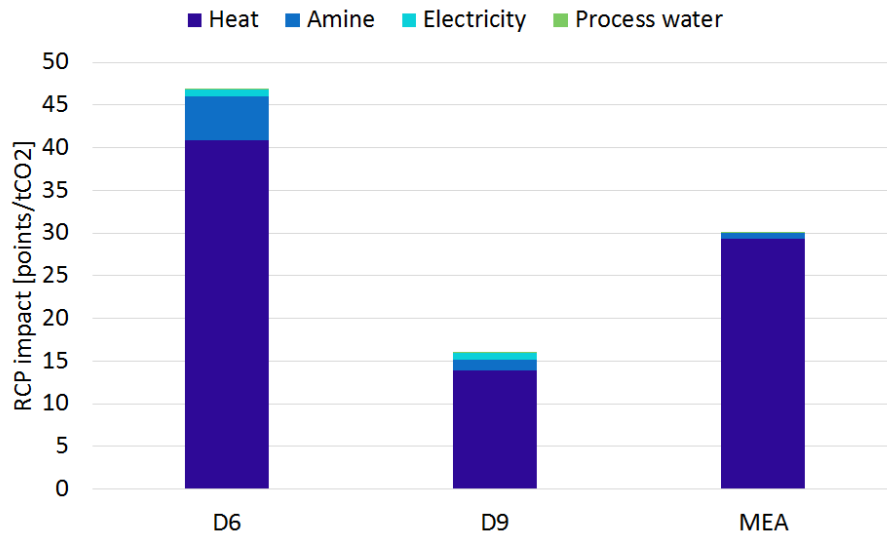


Figure 5.12: ReCiPe points of the base case layouts for D6 and D9 vs MEA scaled to a CO₂ capture capacity of one tonne per hour.

In Figure 5.12 it can be seen that similarly to the other indicator used, D9 provides the least environmental impact and D6 the most with the heat need in the stripper accounting for most of the environmental impact. The layout changes, reduce the points per tonne of CO₂ as expected due to the lower reboiler duty in the stripper, with Layout 1 for D6 being slightly better than MEA and Layout 2 being slightly worse. As in both the CED and the GWP assessment, all layout flowsheets for D9 result in fewer points and thus less environmental impact than both D6 and MEA.

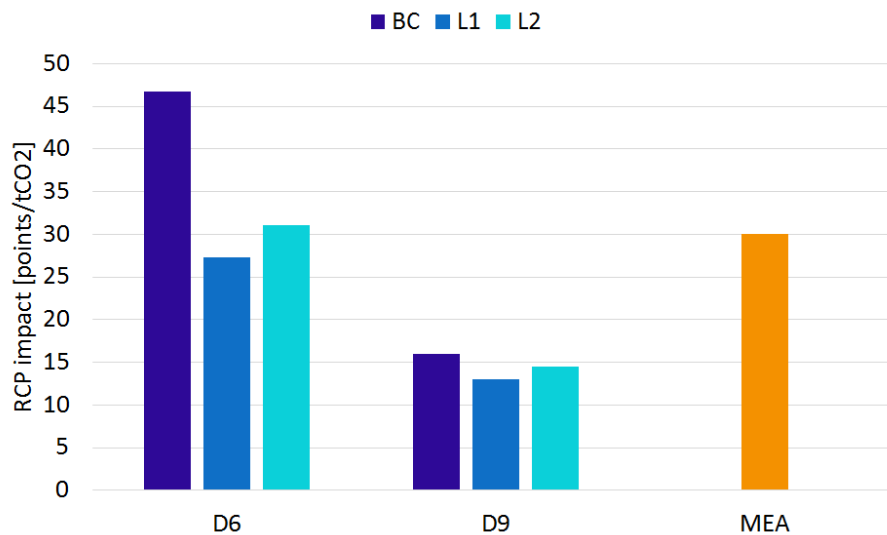


Figure 5.13: ReCiPe points of the layouts for D6 and D9 vs MEA scaled to a CO₂ capture capacity of one tonne per hour.

The points for each layout can be seen in Table 5.5 and the contributions from each utility used can be seen in Tables F.9 and F.10 in appendix B.

Table 5.5: The ReCiPe points for D6, D9 and MEA layouts scaled to a CO₂ capture capacity of one tonne per hour.

	RCP D6	RCP D9	RCP MEA
Base case	46.78	15.95	30.04
Layout 1	27.35	13.00	
Layout 2	31.04	14.51	

5.2.4 Regeneration Energy Requirement

From previous indicators and from the cost assessment it can be seen that the reboiler duty in the stripper is the major factor for both the cost and the environmental impact. So an easy and quick method for determining the efficiency of the different solvents used in this project and solvents that will be used in future work is to compare the regeneration energy requirement for the solvent regeneration in the stripper. This energy requirement can be seen in Table 5.6 for D6, D9 and MEA and their respective layouts.

Table 5.6: The regeneration energy requirement in GJ/tCO₂ of the different flow-sheet layouts.

	D6 [GJ/tCO ₂]	D9 [GJ/tCO ₂]	MEA [GJ/tCO ₂]
Base case	5.31	1.74	3.67
Layout 1	2.79	1.46	
Layout 2	3.21	1.56	

This analysis showed that the layout and solvent with the lowest regeneration energy demand is D9, Layout 1 and the highest solvent was the base case of D6. One of the main goals of the project was to find a process with a regeneration energy demand below 2.0 GJ/tCO₂ captured. This was achieved when using D9 where the lowest regeneration energy demand was for Layout 1. In this case the regeneration required as little as 1.46 GJ/tCO₂ captured which is a significant improvement to the 3.67 GJ/tCO₂ of the reference MEA case.

6

Conclusion

From the results presented in this thesis it is evident that of the solvents tested, D9 is the solvent with the most beneficial properties for performing CCS. It is not only more efficient than D6 but also presents better results than the MEA reference case in all categories but the capital cost, which is however not very different. The most promising results were obtained for flowsheet layout L1 which has an operating cost of 30.10 EUR/tCO₂ captured, a reduction of over 37% compared to the MEA process. All three environmental indicators used (Cumulative Energy Demand, Global Warming Potential and ReCiPe) all point to the processes using D9 being more environmentally friendly than MEA. The primary advantage of D9 is the significantly lower heat requirement in the stripper reboiler which reduces both cost as well as environmental impact of the process compared to D6 and MEA. The results for D6 are not as promising as for D9, which is mostly due to the high reboiler duty of the D6 processes. When using flowsheet Layout 1 the reboiler duty is decreased also for D6 bringing all environmental metrics to levels lower than for MEA, although not as low as D9. However the operating cost is still high which is due to the high price of D6 offsetting the benefits of reduced heat demand.

One of the main goals of the project was to find a process with a regeneration energy demand below 2.0 GJ/tCO₂ captured. This was achieved when using D9 where the lowest regeneration energy demand was for Layout 1. In this case the regeneration required as little as 1.46 GJ/tCO₂ captured which is a significant improvement to the 3.67 GJ/tCO₂ of the reference MEA case.

The sensitivity analyses also provided interesting results. When using equilibrium calculations for the absorber and stripper columns the results for both D6 and D9 showed a discrepancy of around 1% compared to the original results using rate-based calculations. This is very exciting as the simulation time could be significantly reduced while still achieving accurate results when using equilibrium calculations.

Most of the sensitivity analyses showed little impact on the results as most analyses were within 5% of the base case results. Using either vapour-liquid-liquid or liquid-liquid ternary diagrams to represent the decanter phase equilibrium had little effect on the results. This indicates that the question is not which of these most accurately depicts the real behaviour of the mixture, but rather if any of them do and how large impact the chemistry has on the physical equilibrium in the decanter.

The largest uncertainty seems to be the representation of the reactions in the system.

Changing the chemical equilibrium constant of the carbamate formation reaction had considerable impacts on the CO₂ capture capacity and the energy demand of the processes. Experimentally confirmed data for the equilibrium constant could significantly improve the accuracy of the results. It is also worth considering using kinetic reactions instead of equilibrium reactions to further improve accuracy.

6.1 Future work

Any future work on phase changing molecules for CCS should include experimentation to deduce the reaction equilibrium constants for the phase changing molecules and in general to more accurately describe the phase equilibrium of the reacting system. This is of importance as it is one of the largest uncertainties that this project handled. If an experimental method or calculation method for the equilibrium constants could be found, many different molecules could be tested to determine the best possible solvent for CO₂ capture.

Furthermore, the study finding more and better phase changing solvents could be improved by automating the process of the flowsheet configurations. Currently the split fractions used in the decanter had to be manually calculated for each molecule. If programmed into Aspen, this could more quickly try many more molecules to determine the best possible solvent. Additionally, the flowsheeting process could be optimised further using equilibrium based calculations in the absorber and stripper. Using this would drastically reduce computational time without affecting the results by a large factor as can be seen from the sensitivity analyses performed in this project.

By producing a property model in Aspen which could simulate the phase changing behaviour of the molecules while taking the chemistry into account, the accuracy of the simulations could be severely improved. This could possibly make the manual split fraction calculations obsolete since the decanter unit in Aspen, might be able to solve the phase splitting.

So if the process could be made more accurate and reduce the requirement of manual inputs, the programme could quickly and rigorously find the best possible solvent and produce the most efficient carbon capture.

Solvent make up is one of the factors that most influences the operating cost of the processes and more accurate estimations of the solvent degradation and the solvent recovery is therefore necessary to get more accurate predictions of the operating cost. Waste water treatment of the sludge with the degradation products after the solvent reclaimer also affect the environmental impact of the processes making more rigorous studies of the degradation and solvent recovery all the more interesting.

Bibliography

- [1] The United Nations, “Paris agreement,” 2015.
- [2] OECD and IEA, *Energy Technology Perspectives 2016 - Towards Sustainable Urban Energy Systems*. IEA Publications, 2016.
- [3] J. N. Knudsen, J. N. Jensen, P.-J. Vilhelmsen, and O. Biede, “Experience with CO₂ capture from coal flue gas in pilot-scale: Testing of different amine solvents,” *Energy Procedia*, vol. 1, no. 1, pp. 783 – 790, 2009.
- [4] H. Herzog and D. Golomb, “Carbon Capture and Storage from Fossil Fuel Use,” *Encyclopedia of Energy*, vol. 1, pp. 277–287, 2004.
- [5] S. O. Gardarsdottir, F. Normann, K. Andersson, and F. Johnsson, “post-combustion co₂ capture using monoethanolamine and ammonia solvents: The influence of the co₂ concentration on the technical performance,” *Industrial & Engineering Chemistry Research*, vol. 54, pp. 681–690, 2015.
- [6] B. Buhre, L. Elliott, C. Sheng, R. Gupta, and T. Wall, “Oxy-fuel combustion technology for coal-fired power generation,” *Progress in Energy and Combustion Science*, vol. 31, no. 4, pp. 283 – 307, 2005.
- [7] P. Broutin, “Pre-combustion CO₂ capture,” *The Oil and Gas Engineering Guide*, pp. 111 – 112, 2010.
- [8] R. Svensson, M. Odenberger, F. Johnsson, and L. Strömberg, “Transportation systems for CO₂-application to carbon capture and storage,” *Energy Conversion and Management*, vol. 45, no. 15–16, pp. 2343 – 2353, 2004.
- [9] National Energy Technology Laboratory & U.S. Department of Energy, “Carbon Dioxide Enhanced Oil Recovery - Untapped Domestic Energy Supply and Long Term Carbon Storage Solution,” tech. rep., U.S. Department of Energy Office of Fossil Fuels, 2010.
- [10] R. Chadwick, “10 - Offshore CO₂ storage: Sleipner natural gas field beneath the North Sea,” in *Geological Storage of Carbon Dioxide (CO₂)* (J. Gluyas, , and S. Mathias, eds.), pp. 227 – 253e, Woodhead Publishing, 2013.
- [11] S. Benson *et al.*, “5 - Underground geological storage,” in *IPCC Special Report on Carbon Dioxide Capture and Storage* (B. Metz, O. Davidson, H. de Coninck, M. Loos, and L. Meyer, eds.), Cambridge University Press, 2005.

- [12] K. Caldeira *et al.*, “6 - Ocean storage,” in *IPCC Special Report on Carbon Dioxide Capture and Storage* (B. Metz, O. Davidson, H. de Coninck, M. Loos, and L. Meyer, eds.), Cambridge University Press, 2005.
- [13] M. Mazzotti *et al.*, “7 - Mineral carbonation and industrial uses of carbon dioxide,” in *IPCC Special Report on Carbon Dioxide Capture and Storage* (B. Metz, O. Davidson, H. de Coninck, M. Loos, and L. Meyer, eds.), Cambridge University Press, 2005.
- [14] R. Robert, “Process for separating acidic gases,” 1930. US Patent 1,783,901.
- [15] A. B. Rao, E. S. Rubin, and M. B. Berkenpas, “An Integrated Modeling Framework for Carbon Management Technologies - Volume 1 - Technical Documentation: Amine Based CO₂ Capture and Storage Systems for Fossil Fuel Power Plant,” tech. rep., C.M.U. Department of Engineering and Public Policy, 2004.
- [16] V. Darde, K. Thomsen, W. J. van Well, and E. H. Stenby, “Chilled ammonia process for CO₂ capture,” *International Journal of Greenhouse Gas Control*, vol. 4, no. 2, pp. 131–136, 2010. The Ninth International Conference on Greenhouse Gas Control Technologies.
- [17] A. Bandyopadhyay, “Amine versus ammonia absorption of CO₂ as a measure of reducing GHG emission: a critical analysis,” *Clean Technologies and Environmental Policy*, vol. 13, no. 2, pp. 269–294, 2011.
- [18] H. Herzog, J. Meldon, and A. Hatton, “Advanced post-combustion CO₂ capture,” *Clean Air Task Force*, p. 39, 2009.
- [19] E. Gal, “Ultra cleaning combustion gas including the removal of CO₂,” 2006. Patent WO 2006022885.
- [20] J. Gaspar, M. W. Arshad, E. A. Blaker, B. Langseth, T. Hansen, K. Thomsen, N. von Solms, and P. L. Fosbøl, “A Low Energy Aqueous Ammonia CO₂ Capture Process,” *Energy Procedia*, vol. 63, pp. 614–623, 2014.
- [21] S. A. Bedell, “Oxidative degradation mechanisms for amines in flue gas capture,” *Energy Procedia*, vol. 1, no. 1, pp. 771 – 778, 2009. Greenhouse Gas Control Technologies 9 - Proceedings of the 9th International Conference on Greenhouse Gas Control Technologies (GHGT-9), 16–20 November 2008, Washington DC, USA.
- [22] D. Cringle, R. Pearce, and M. Dupart, “Method for maintaining effective corrosion inhibition in gas scrubbing plant,” Sept. 1 1987. US Patent 4,690,740.
- [23] A. K. Voice, *Amine oxidation in carbon dioxide capture by aqueous scrubbing*. PhD thesis, The University of Texas at Austin, May 2013.
- [24] S. Badr, *Sustainability Assessment of Amine-based Post Combustion CO₂ Capture*. PhD thesis, ETH Zurich, 2016.
- [25] A. Reynolds, T. Verheyen, and E. Meuleman, “16 - Degradation of amine-based solvents,” in *Absorption-Based Post-combustion Capture of Carbon Diox-*

- ide* (P. H. Feron, ed.), pp. 399 – 423, Woodhead Publishing, 2016.
- [26] G. S. Goff and G. T. Rochelle, “Monoethanolamine Degradation: O₂ Mass Transfer Effects under CO₂ Capture Conditions,” *Industrial & Engineering Chemistry Research*, vol. 43, no. 20, pp. 6400–6408, 2004.
- [27] J. Davis, *Thermal degradation of aqueous amines used for carbon dioxide capture*. Ph.d. dissertation, University of Texas at Austin, 2009.
- [28] Aspen Technology Inc., *Aspen Physical Property System - Physical Property Methods*, 2013.
- [29] C. C. Chen, H. I. Britt, J. F. Boston, and L. B. Evans, “Local Composition Models for Excess Gibbs Energy of Electrolyte Systems,” *AIChE Journal*, vol. 28, pp. 588–596, 1982.
- [30] A. Fredenslund, R. L. Jones, and J. M. Prausnitz, “Group-contribution estimation of activity coefficients in nonideal liquid mixtures,” *AIChE Journal*, vol. 21, no. 6, pp. 1086–1099, 1975.
- [31] A. I. Papadopoulos *et al.*, “Computer-aided molecular design and selection of CO₂ capture solvents based on thermodynamics, reactivity and sustainability,” *Mol. Syst. Des. Eng.*, vol. 1, pp. 313–334, 2016.
- [32] Aspen Technology Inc., *Aspen Physical Property System - Physical Property Data*, 11.1 ed., 2001.
- [33] J. Gmehling, J. Lohmann, A. Jakob, J. Li, and R. Joh, “A Modified UNI-FAC (Dortmund) Model. 3. Revision and Extension,” *Industrial & Engineering Chemistry Research*, vol. 37, no. 12, pp. 4876–4882, 1998.
- [34] M. Aleixo *et al.*, “Physical and chemical properties of DMX™ solvents,” *Energy Procedia*, vol. 4, pp. 148 – 155, 2011.
- [35] L. Kucka, I. Müller, E. Y. Kenig, and A. Górak, “On the modelling and simulation of sour gas absorption by aqueous amine solutions,” *Chemical Engineering Science*, vol. 58, no. 16, pp. 3571 – 3578, 2003.
- [36] Sulzer Corporation, *Structured Packings - Energy-efficient, innovative and profitable*, 15 ed.
- [37] B. A. Oyenekan and G. T. Rochelle, “Alternative stripper configurations for CO₂ capture by aqueous amines,” *AIChE Journal*, vol. 53, no. 12, pp. 3144–3154, 2007.
- [38] R. Zevenhoven and P. Kilpinen, *Control of pollutants in flue gases and fuel gases*. Picaset Oy, Espoo, 2001. <http://users.abo.fi/rzevenho/gasbook.html>.
- [39] EIA, “Carbon emission coefficients.” https://www.eia.gov/environment/emissions/co2_vol_mass.cfm.
- [40] OECD and IEA, *Power Generation from Coal - Measuring and Reporting Ef-*

- iciency Performance and CO2 Emissions*. IEA Publications, 2010.
- [41] U.S. Energy Information Administration, “Capital Cost Estimates for Utility Scale Electricity Generating Plants,” 2016. https://www.eia.gov/analysis/studies/powerplants/capitalcost/pdf/capcost_assumption.pdf.
- [42] XE Currency Converter, “USD to EUR.” <http://www.xe.com/currencyconverter/convert/?From=USD&To=EUR>, Retrieved on: 2017-05-12.
- [43] Ecoinvent, “Ecoinvent v. 3.3.”
- [44] Molbase, “3,3'-iminobis(n,n-dimethylpropylamine).” CAS [6711-48-4], <http://www.molbase.com/en/cas-6711-48-4.html>, Retrieved on: 2017-05-19.
- [45] Molbase, “2-(2-aminoethylamino)ethanol.” CAS [111-41-1], <http://www.molbase.com/en/cas-111-41-1.html>, Retrieved on: 2017-05-19.
- [46] V. D. Ingenieure, “Cumulative energy demand—terms, definitions, methods of calculation,” *VDI-Richtlinien 4600*, 2012.
- [47] M. J. Elrod, “Greenhouse Warming Potentials from the Infrared Spectroscopy of Atmospheric Gases,” *Journal of Chemical Education*, vol. 76, no. 12, p. 1702, 1999.
- [48] M. Goedkoop *et al.*, “ReCiPe 2008 - A life cycle impact assessment method which comprises harmonised category indicators at the midpoint and the endpoint level,” tech. rep., Ministry of Housing, Spatial Planning and Environment, Netherlands, 2013.
- [49] O. Redlich and J. N. S. Kwong, “On the Thermodynamics of Solutions V - An Equation-of-state. Fugacities of Gaseous Solutions,” *Chemical Reviews*, vol. 44, pp. 223–244, 1949.

A

Equations related to the property methods

ELECNRTL

The ELECNRTL method uses a sum of the long range and short range contributions to calculate the molar excess Gibbs free energy.

$$\frac{g^{ex*}}{RT} = \frac{g^{ex*,LR}}{RT} + \frac{g^{ex*,SR}}{RT} \quad (\text{A.1})$$

These are calculated as follows:

Long range contribution

The long range interaction contribution to the molar excess Gibbs free energy are also supplied by the extended Debye-Hückel equation proposed by Pitzer as the true mole fraction is taken into account as well as the repulsive forces. The expression for the normalised Pitzer-Debye-Hückel is

$$g^{ex*,PDH} = - \left(\sum_k x_k \right) \left(\frac{1.000}{M_W} \right)^{1/2} \left(\frac{4A_\phi I_x}{\rho} \right) \ln \left(1 + \rho I_x^{1/2} \right) \quad (\text{A.2})$$

for all species k and where x_k is the liquid phase mole fraction, M_W is the molecular weight of the solvent, ρ is the "closest approach" parameter and I_x and A_ϕ are the ionic strength and the Debye-Hückel parameter respectively given by

$$A_\phi = \frac{1}{3} \left(\frac{2\pi N_0 d}{1000} \right)^{1/2} \left(\frac{e^2}{D_w k_B T} \right)^{3/2} \quad (\text{A.3})$$

where N_0 is the Avogadro's number, d is the solvent density, e is the charge of an electron, D_w is the dielectric constant of water, k_B is the Boltzmann constant and T is the temperature, and

$$I_x = \frac{1}{2} \sum Z_k^2 x_k \quad (\text{A.4})$$

where Z_k is the charge of the species k .

This case is only representative when the ionic species is diluted in a mixed solvent. The ELECNRTL method however uses ionic species diluted in water. Thus the Born expression is used as a correction of this.

$$g^{ex*,LR} = g^{ex*,PDH} + g^{ex*,Born} \quad (\text{A.5})$$

The equation for $g^{ex*,Born}$ is given by

$$g^{ex*,Born} = RT \left(\frac{e^2}{2k_B T} \right) \left(\frac{1}{D_S} - \frac{1}{D_w} \right) \left(\sum_k \frac{Z_k^2 x_k}{r_k} \right) 10^{-2} \quad (\text{A.6})$$

where D_s is the dielectric constant of the solvent and r_k is the Born radius of the species k .

Short range contribution

Short range or local contribution uses the Non-Random Two-Liquid (NRTL) model to calculate the molar excess Gibbs free energy. This model was proposed by Renon and Prausnitz and was adopted by the ELECNRTL models as it is based on the assumption of negligible non-ideal entropy of mixing. This is accurate for electrolyte systems as the heat of mixing is very large and thus the non-ideal entropy of mixing can be disregarded. The short range contributions are defined by

$$\begin{aligned} g^{ex*,SR} = & \left(\sum_m X_m \frac{\sum_j X_j G_{jm} \tau_{jm}}{\sum_k X_k G_{km}} \right) \\ & + \sum_c X_c \sum_{a'} \frac{X_{a'} \sum_j G_{jc,a'c} \tau_{jc,a'c}}{\left(\sum_{a''} X_{a''} \right) \left(\sum_k X_k G_{kc,a'c} \right)} + \dots \\ & + \dots + \sum_a X_a \sum_{c'} \frac{X_{c'} \sum_j G_{ja,c'a} \tau_{ja,c'a}}{\left(\sum_{c''} X_{c''} \right) \left(\sum_k X_k G_{ka,c'a} \right)} \end{aligned} \quad (\text{A.7})$$

Vapour phase calculations

The ELECNRTL model used the Redlich-Kwong (RK) equation of state for all vapour phase calculations. The RK equation of state calculates thermodynamic properties in the vapour phase at moderate pressure using the following equation[49]:

$$P = \frac{RT}{V_m - b} - \frac{a/T^{0.5}}{V_m(V_m + b)}, \quad (\text{A.8})$$

where

$$\sqrt{a} = \sum_i x_i \sqrt{a_i} \quad \text{and} \quad a_i = 0.42748023 \frac{R^2 T_{c,i}^{1.5}}{P_{c,i}} \quad (\text{A.9})$$

and

$$b = \sum_i x_i b_i \quad \text{and} \quad b_i = 0.08664035 \frac{RT_{c,i}}{P_{c,i}} \quad (\text{A.10})$$

where V_m is the molar volume, R is the ideal gas constant, $T_{c,i}$ is the critical temperature for component i and $P_{c,i}$ is the critical pressure for component i .

UNIQUAC Functional-group Activity Coefficient

The UNIFAC property method uses group contributions to calculate the binary parameters for the activity coefficients used. It calculates these contributions as a sum of the combinatorial and the residual activity coefficients. The combinatorial activity contribution is the same as that for the UNIQUAC model:

$$\ln \gamma_i^c = \ln \frac{\psi_i}{x_i} + \frac{z}{2} q_i \ln \frac{\theta_i}{\psi_i} + L_i - \frac{\psi_i}{x_i} \sum_{j=1}^n x_j L_j \quad (\text{A.11})$$

where θ_i is the molar weighted segment of component i , ψ_i is the area fractional component of component i and L_i is the compound parameter. These are calculated using the following correlations:

$$\theta_i = \frac{x_i q_i}{\sum_{j=1}^n x_j q_j} \quad ; \quad \psi_i = \frac{x_i r_i}{\sum_{j=1}^n x_j r_j} \quad ; \quad L_i = \frac{z}{2} (r_i - q_i) - (r_i - 1) \quad (\text{A.12})$$

r_i and q_i are contributions from the group surface area (Q) and volume (R), usually calculated from tabulated values and are dependent on the number of occurrence of the functional group, ν_i .

$$r_i = \sum_{k=1}^n \nu_k R_k \quad ; \quad q_i = \sum_{k=1}^n \nu_k Q_k \quad (\text{A.13})$$

The contributions of the individual group interactions are defined by the residual component of the activity coefficient:

$$\ln\gamma_i^r = \sum_k^n \nu_k^{(i)} \left(\ln\Gamma_k - \ln\Gamma_k^{(i)} \right) \quad (\text{A.14})$$

This defined the interaction of molecule i which consists of n unique functional groups. $\ln\Gamma_k$ and $\ln\Gamma_k^{(i)}$ are calculated using the following equation:

$$\ln\Gamma_k = Q_k \left(1 - \ln \sum_m \Theta_m \Psi_{mk} - \sum_m \frac{\Theta_m \Psi_{km}}{\sum_n \Theta_n \Psi_{nm}} \right) \quad (\text{A.15})$$

In this equation, Θ_m is the sum of the area fraction of group m , Ψ_{mn} is the group interaction parameter and X_n is the group mole fraction. These parameters are calculated as shown by the equations seen below.

$$\Theta_m = \frac{Q_m X_m}{\sum_n Q_n X_n} \quad ; \quad \Psi_{mn} = \exp\left(-\frac{U_{mn} - U_{nm}}{RT}\right) \quad ; \quad X_m = \frac{\sum_j \nu_m^j x_j}{\sum_j \sum_n \nu_n^j x_j} \quad (\text{A.16})$$

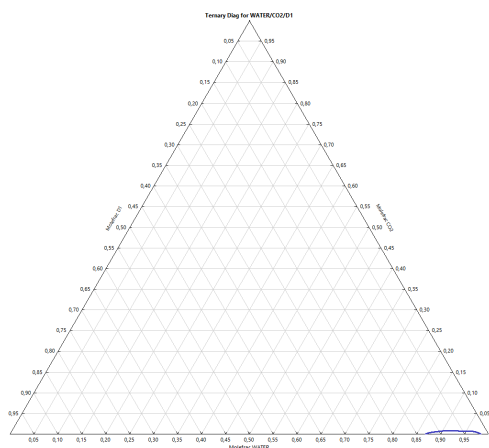
Where U_{mn} is the energy of interaction between group m and group n and vice versa for U_{nm} .

B

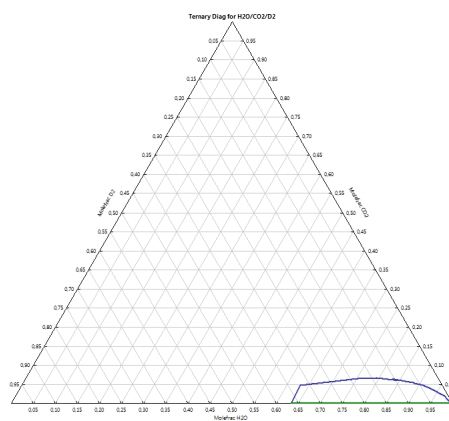
Ternary diagrams for all design molecules tested

Ternary diagram could not be produced for all design molecules as they according to Aspen did not exhibit the phase changing behaviour. The molecules that did are presented below.

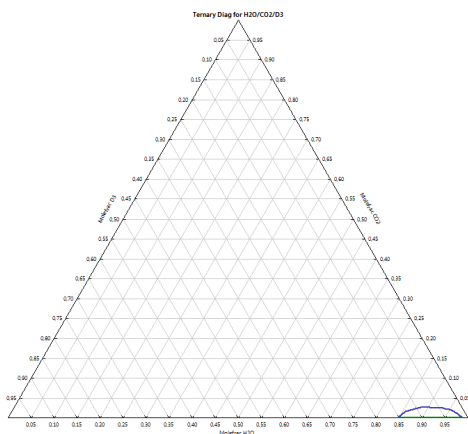
B. Ternary diagrams for all design molecules tested



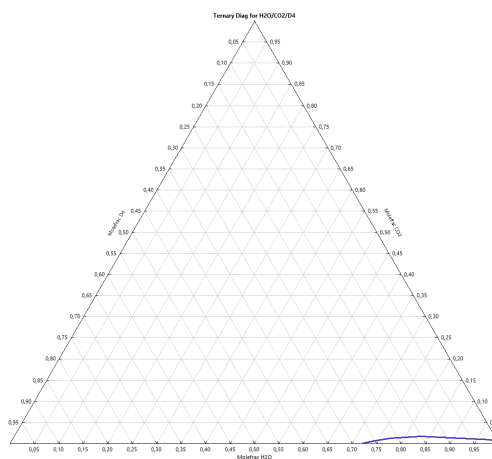
(a) Ternary diagram for the D1/water/CO₂ mixture



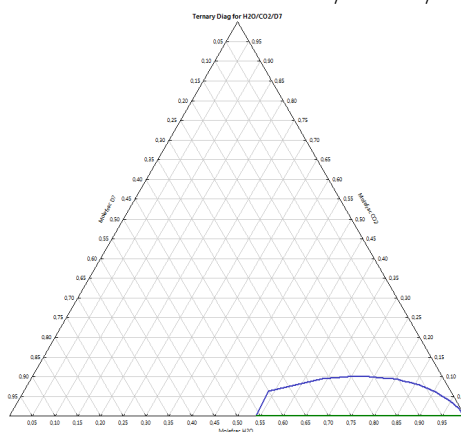
(b) Ternary diagram for the D2/water/CO₂ mixture at 2 bar



(c) Ternary diagram for the D3/water/CO₂ mixture at 10 bar



(d) Ternary diagram for the D4/water/CO₂ mixture at 2 bar



(e) Ternary diagram for the D7/water/CO₂ mixture at 2 bar

Figure B.1: VLE ternary diagrams estimated by Aspen for the remaining design molecules not chosen for the project.

C

Calculations of VLL equilibrium

The calculations for the VLL equilibrium were done as described below.

The total material balance of the decanter was written as:

$$F = L + R \quad (\text{C.1})$$

where F is the feed stream to the decanter, L is the CO₂-lean stream and R is the CO₂-rich stream leaving the decanter.

The component balance of the decanter was written as:

$$Fx_F(i) = Lx_L(i) + Rx_R(i) \quad (\text{C.2})$$

where $x_j(i)$ is the molar fraction of component i in stream j .

The only components considered in the decanter are water, amine and CO₂ that is physically absorbed in the liquid phase. The molar fraction of the amine was determined in apparent components and thus the ionic forms of the amine are treated like the molecular form assuming that they will behave identically. The feed composition x_F was obtained from the Aspen simulation and the rich and lean compositions, x_R and x_L respectively, were read from the tie lines in the ternary diagram.

The vapour-liquid-liquid equilibrium ternary diagram at atmospheric pressure is shown in figure C.1 for the different design molecules.

C. Calculations of VLL equilibrium

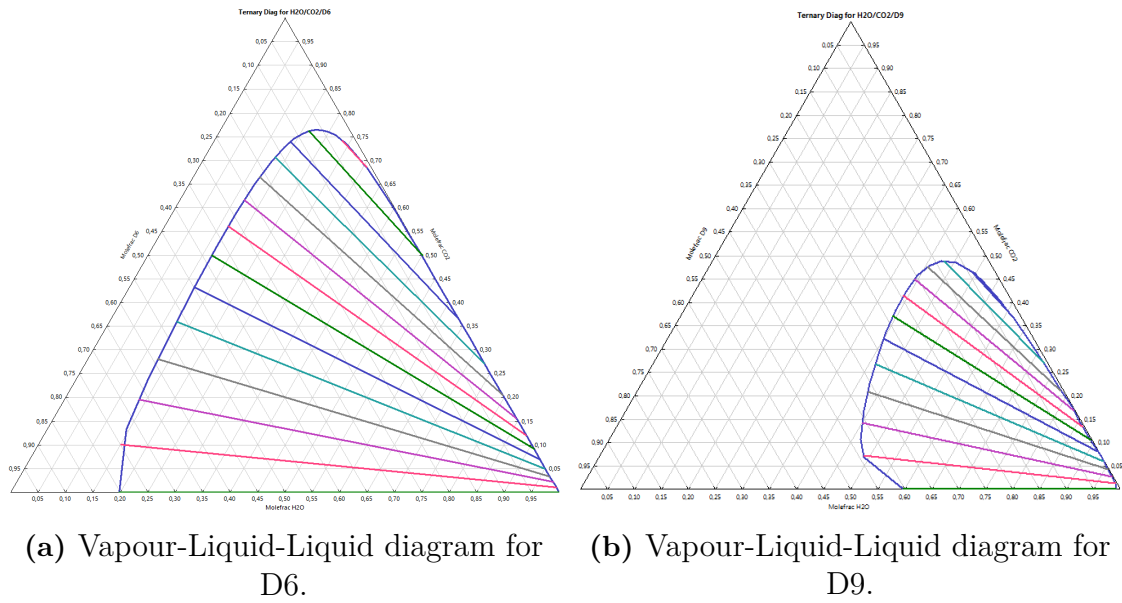


Figure C.1: The Vapour-Liquid-Liquid diagrams for amine/water/CO₂ mixture at atmospheric pressure.

By combining and rewriting equations (C.1) and (C.2) the molar flow of the rich stream was calculated using equation (C.3). The lean stream molar flow was then obtained using equation (C.1).

$$R = F \frac{x_F(i) - x_L(i)}{x_R(i) - x_L(i)} \quad (C.3)$$

The split fractions to the lean stream for each component could then be determined using equation (C.4).

$$\alpha_L(i) = \frac{Lx_L(i)}{Fx_F(i)} \quad (C.4)$$

D

Setup of units in Aspen Plus

A detailed description of how the major units of the CCS setup in Aspen plus will be described here:

Absorber

The absorber was chosen as a *RadFrac* column and in order to achieve the most accurate results possible the *Calculation type* of the column was set to **Rate-Based**. The *Number of stages* was set to **20** and gave for our calculations, a suitable height for the column. The absorber was set up to have no condenser or reboiler.

The feed streams were set by placing the flue gas stream in the bottom of the absorber and the solvent in the top, ie. the flue gases on stage **20** and the solvent on stage **1**. Under *Pressure* in the *Specifications* sheet, the *Top stage* pressure was set to **1.01325 bar** with no pressure drop over the column in order to simplify calculations.

When choosing rate-based calculations, packing or trays need to be included. For these calculations, *Packing Rating* was chosen and a new packing section was chosen. The *Starting stage* was set to **1** and the *Ending stage* to **20**. The *Type* of packing was chosen as **MELLAPAK** from the *Vendor Sulzer*, *Material* used as **STANDARD** and *Dimensions* **250Y**. As a starting guess, the *Section diameter* was set to **5.5 meters** and the *Section packed height* was set to **30 meters**.

Under the *Packing Rating* tab for the section chosen, changes in the *Rate-based* sheet was made. Firstly the *Rate-based calculations* box was checked. Under *Film resistance*, *Liquid phase - Discrxn* and *Vapor phase - Film* were selected. Then in the *Design* tab the box for *Design mode to calculate column diameter* was checked, the *Base stage* was set to **2** and the *Base flood* was chosen as **0.7**. Under *Optional* 8 discretization points were added at the distances shown in table 4.3.

Furthermore the Absorber was further changed under the *Convergence* tab, where *Temperature estimates* were set on stage 2, 10 and 15. These estimates varied between the cases, but in the range of 40-80 °C. Under *Convergence/Convergence/Advanced* the *Absorber* setting was set to **Yes**.

Decanter

The decanter setup was not done using the built-in decanter block in Aspen Plus but was chosen as a simple *Sep* block where the *Outlet stream conditions* were changed according to the VLL equilibrium calculated in Appendix C. Other than changing the split fractions no other changes were made to the *Sep* block.

Stripper

The stripper was also modeled as a *RadFrac* using **Rate-Based** calculations as the *Calculation type*. In the stripper, the *Number of stages* were again set to **20** with no condenser and a **Kettle** reboiler as the *Reboiler*. Under *Operating specifications* the **Reboiler duty** was selected and set to a value between 35 and 55 MW for the flow rates used in these calculations.

The feed streams were for the stripper the inlet as well as a reflux stream of which both were set to enter the column on stage **1**. The *Pressure* was set to **2 bar** and no changes were made to the *Reboiler*.

The same material as for the absorber was chosen for the *Packing Rating* of the stripper. Here due to the reboiler, the *Starting stage* was set to **1** and the *Ending stage* to **19**. The *Section diameter* was first guessed as **5 meters** and the *Section packed height* was set to **15 meters**.

The same changes as in the absorber were made under the *Rate-Based* sheet for the stripper, using the same discretization points and *Design* options.

For flowsheets needing help with convergence, higher *Temperature estimates* were supplied, than those for the absorber and were in the range of 100-140 °C for stages 2, 10 and 18. Under *Convergence/Convergence/Advanced* the *Absorber* setting was set to **Yes** for the stripper as well.

Flashes

The flashes used in the simulations were setup using the *Flash specifications* **Duty** and **Pressure**, where the duty was set to **0**, and the pressure to the same as the inlet, in order to avoid energy usage and only flash the inlet stream.

Heating, cooling and heat exchanging

The heat exchanging performed in these simulations have been chosen to use a ΔT_{min} of 5 °C and was set up by connecting a heater and a cooler using a heat

stream in Aspen Plus and the pressure drop over the heaters or coolers was set to be zero.

E

Purge calculations

To calculate the required flowrate of the purge stream material balances over the stripper and the mixing point as indicated in figure 4.10

Material balance over the stripper:

$$c_1 L_1 = c_2 L_2 (1 - \alpha) + \dot{m}_d \quad (\text{E.1})$$

Material balance over the mixing point:

$$c_2 L_2 = c_1 L_1 - c_1 P + c_2 L_2 \alpha \quad (\text{E.2})$$

L_1 is the mass flow rate in kg/hr of the lean amine stream leaving the stripper and c_1 is the concentration in wt% of degradation products present in the stream. The amount of degradation products is thus $c_1 L_1$. The amount of degradation products in the stream to the reclaimer unit is $c_1 P$ and the amount both entering and exiting the absorber is $c_2 L_2$. The rate at which degradation products are formed, \dot{m}_d is measured in kg/hr.

Rearranging equation D.2 gives the following expression:

$$c_2 = \frac{c_1(L_1 - P)}{L_2} \cdot \frac{1}{(1 - \alpha)} \quad (\text{E.3})$$

Substituting c_1 in equation D.3 with the expression from D.1 and solving for P/L_1 results in

$$\frac{P}{L_1} = \frac{\dot{m}_d}{c_2 L_2 (1 - \alpha) + \dot{m}_d} \quad (\text{E.4})$$

where P/L_1 is the purge factor, the fraction of L_1 that is sent to the reclaimer unit.

In the reclaimer unit the degradation products are removed and most of the solvent can be recovered. Assuming a 5wt% loss of the solvent sent to the reclaimer, the total loss of amine was calculated as

$$\dot{m}_{\text{purge}} = \dot{m}_d \left(1 + 0.05 \frac{\dot{m}_{L_1}^{\text{amine}}}{\dot{m}_d + c_2 L_2 (1 - \alpha)} \right) \quad (\text{E.5})$$

In Layout 2 with the double matrix stripper configuration, the purge factor was determined by assuming equal concentrations of degradation products in the semi-lean and lean streams leaving the lower pressure stripper. The equation was then modified to the following expression:

$$\frac{P}{(L_1 + SL_1)} = \frac{\dot{m}_d}{c_2 L_2 (1 - \alpha) + \dot{m}_d} \quad (\text{E.6})$$

where the new purge factor is $P/(L_1 + SL_1)$, L_1 and SL_1 are the mass flow rate in kg/hr of the lean and semi-lean amine leaving the lower pressure stripper.

F

Detailed results of the economic and environmental assessments

F.1 Economic assessment

Detailed results from the economic assessment is included in this appendix.

Table F.1: Capital cost estimations of the D6, D9 and MEA flowsheets performed in Aspen given in USD unless specified.

	D6	D9	MEA base
HEX 1	590 600	139 600	792 600
HEX 2	876 400	217 600	
Cooler 1	27 000	15 200	76 300
Cooler 2	592 000	645 000	81 600
Flash 1	211 200	115 300	22 700
Flash 2	26 900	26 200	-
Flash 3	213 800	115 000	-
Decanter	120 300	86 100	-
Pump 1	79 600	30 400	22 600
Pump 2	7 200	5 100	-
Compressor	2 034 700	2 033 900	-
Absorber	9 722 700	8 087 400	6 596 200
Stripper	859 100	212 300	248 000
Reboiler	957 700	720 100	1 270 100
Total	16 319 200	12 449 200	9 110 100
Total [EUR]	15 021 318	11 459 103	8 385 565
Total cost/MW [EUR]	185 859	141 783	131 358

Table F.2: Yearly operating cost for the D6 process in EUR.

	Heat	Electricity	Process water	Amine	Total Cost	CO ₂ captured [kmol/hr]	Cost/tCO ₂
Base case	35 939 100	840 220	21 683	29 535 789	66 336 792	1 414	133.21
Layout 1	19 477 348	96 918	18 979	29 393 524	48 986 769	1 415	98.33
Layout 2	22 377 600	846 473	22 492	29 646 610	52 893 174	1 415	106.17
Scenario 1	35 785 957	839 438	22 757	29 531 988	66 180 141	1 415	132.84
Scenario 2	36 177 996	839 438	21 682	29 512 012	66 551 129	1 415	133.58
Scenario 3	36 033 918	805 830	21 678	29 547 752	66 409 177	1 415	133.30
Scenario 4	64 512 000	917 598	20 080	29 310 676	94 760 354	1 400	192.25
Scenario 5	25 718 149	805 048	39 377	28 544 803	55 107 377	1 416	110.57
Scenario 6	37 363 568	839 438	21 682	29 516 324	67 741 012	1 415	135.97
Scenario 7	33 971 277	847 254	21 691	29 792 018	64 632 240	1 415	129.73
Scenario 8	36 604 847	846 473	21 690	27 807 052	65 280 061	1 415	131.03

Table F.3: Yearly operating cost for the D9 process in EUR.

	Heat	Electricity	Process water	Amine	Total Cost	CO ₂ captured [kmol/hr]	Cost/tCO ₂
Base case	12 153 960	767 851	35 071	4 672 610	17 629 492	1 415	35.40
Layout 1	10 187 695	31 475	34 335	4 720 203	14 973 708	1 413	30.10
Layout 2	11 088 000	814 572	34 942	4 809 094	16 746 608	1 444	32.93
Scenario 1	12 265 509	761 486	35 503	4 699 773	17 762 272	1 423	35.45
Scenario 2	12 090 662	768 350	35 092	4 685 288	17 579 391	1 415	35.28
Scenario 3	12 102 060	768 603	35 082	4 686 541	17 592 286	1 416	35.29
Scenario 4	10 551 986	810 334	33 101	4 839 667	16 235 088	1 416	32.58
Scenario 5							
Scenario 6	12 742 043	799 527	35 188	4 682 082	18 258 840	1 415	36.66
Scenario 7	11 898 311	799 321	35 035	4 684 851	17 417 518	1 415	34.97
Scenario 8	11 695 703	799 402	35 096	4 706 680	17 236 881	1 415	34.61

Table F.4: Yearly operating cost for the D9 process in EUR.

	Heat	Electricity	Process water	Amine	Total Cost	CO ₂ captured [kmol/hr]	Cost/tCO ₂
MEA	20 147 178	22 367	160 646	1 869 289	22 199 481	1116	56.50

F.2 Environmental assessment

Detailed results from the environmental assessment is included in this appendix.

Table F.5: Yearly cumulative energy demand of the D6 processes in MJ-eq.

	Heat	Electricity	Process water	Amine	Total CED	CO ₂ captured	CED/+CO ₂
Base case	3 080 494 285	95 460 000	13 434	395 481 652	3 571 449 372	1 414	7.1717
Layout 1	1 669 486 993	11 011 200	11 759	393 576 734	2 074 086 685	1 415	7.1422
Layout 2	1 918 080 000	96 170 400	13 935	396 965 532	2 411 229 867	1 415	7.2091
Scenario 1	3 067 367 757	95 371 200	14 099	395 430 757	3 558 183 813	1 415	7.1776
Scenario 2	3 100 971 115	95 371 200	13 433	395 163 285	3 591 519 033	1 400	12.2260
Scenario 3	3 088 621 545	91 552 800	13 431	395 641 828	3 575 829 604	1 416	5.3737
Scenario 4	5 529 600 000	104 251 200	12 441	392 467 404	6 026 331 045	1 415	4.1632
Scenario 5	2 204 412 752	91 464 000	24 397	382 212 439	2 678 113 587	1 415	4.8399
Scenario 6	3 202 591 545	95 371 200	13 434	395 221 009	3 693 197 188	1 415	7.4132
Scenario 7	2 911 823 728	96 259 200	13 439	398 912 532	3 407 008 899	1 415	6.8387
Scenario 8	3 137 558 304	96 170 400	13 438	372 334 007	3 606 076 149	1 415	7.2383

Table F.6: Yearly cumulative energy demand of the D9 processes in MJ-eq.

	Heat	Electricity	Process water	Amine	Total CED	CO ₂ captured [kmol/hr]	CED/+CO ₂
Base case	1 041 768 000	87 237 919	21 729	267 746 793	1 396 774 441	1 415	2.8043
Layout 1	873 230 976	3 575 940	21 273	270 473 944	1 147 302 133	1 413	2.3064
Layout 2	950 400 000	92 546 028	21 649	275 567 521	1 318 535 198	1 444	2.5929
Scenario 1	1 051 329 370	86 514 821	21 997	269 303 256	1 407 169 443	1 423	2.8087
Scenario 2	1 036 342 426	87 294 574	21 742	268 473 254	1 392 131 995	1 415	2.7937
Scenario 3	1 037 319 437	87 323 345	21 736	268 545 065	1 393 209 582	1 416	2.7948
Scenario 4	904 455 936	92 064 536	20 508	277 319 377	1 273 860 357	1 416	2.5560
Scenario 5							
Scenario 6	1 092 175 142	90 836 708	21 801	268 289 551	1 451 323 203	1 415	2.9136
Scenario 7	1 019 855 232	90 813 363	21 707	268 448 203	1 379 138 505	1 415	2.7692
Scenario 8	1 002 488 832	90 822 509	21 744	269 699 052	1 363 032 137	1 415	2.7365

Table F.7: Yearly global warming potential of the D6 processes in kg CO₂-eq.

	Heat	Electricity	Process water	Amine	Total GWP	CO ₂ captured	Net capture	Net CO ₂ per tCO ₂ captured in stripper
Base case	205 366 286	4 128 000	1 155	15 263 078	224 758 519	1 414	278 077 560	0.5530
Layout 1	111 299 133	476 160	1 011	15 189 560	126 965 864	1 415	375 370 261	0.7472
Layout 2	127 872 000	4 158 720	1 198	15 320 347	147 352 264	1 415	361 237 858	0.7103
Scenario 1	204 491 184	4 124 160	1 212	15 261 114	223 877 670	1 415	278 198 973	0.5541
Scenario 2	206 731 408	4 124 160	1 155	15 250 791	226 107 514	1 415	276 075 457	0.5498
Scenario 3	205 908 103	3 959 040	1 155	15 269 260	225 137 558	1 415	276 693 685	0.5514
Scenario 4	368 640 000	4 508 160	1 069	15 146 747	388 295 977	1 400	105 581 426	0.2138
Scenario 5	146 960 850	3 955 200	2 097	14 750 971	165 669 118	1 416	332 702 586	0.6676
Scenario 6	213 506 103	4 124 160	1 155	15 253 019	232 884 437	1 415	269 915 026	0.5368
Scenario 7	194 121 582	4 162 560	1 155	15 395 488	213 680 786	1 415	288 320 160	0.5743
Scenario 8	209 170 554	4 158 720	1 155	14 369 726	227 700 155	1 415	274 538 796	0.5466

Table F.8: Yearly global warming potential of the D9 processes in kg CO₂-eq.

	Heat	Electricity	Process water	Amine	Total GWP	CO ₂ captured [kmol/hr]	Net capture	Net CO ₂ per tCO ₂ captured in stripper
Base case	69 451 200	3 772 451	1 868	10 276 966	83 502 484	1 415	414 567 488	0.8323
Layout 1	58 215 398	154 635	1 829	10 381 643	68 753 505	1 413	428 682 723	0.8612
Layout 2	63 360 000	4 001 990	1 861	10 577 150	77 941 002	1 444	430 568 142	0.8467
Scenario 1	70 088 625	3 741 181	1 891	10 336 708	84 168 405	1 423	416 823 831	0.8320
Scenario 2	69 089 495	3 774 900	1 869	10 304 850	83 171 114	1 415	415 145 314	0.8331
Scenario 3	69 154 629	3 776 145	1 869	10 307 606	83 240 248	1 416	415 255 740	0.8330
Scenario 4	60 297 062	3 981 169	1 763	10 644 392	74 924 386	1 416	423 458 937	0.8497
Scenario 5								
Scenario 6	72 811 676	3 928 074	1 874	10 297 799	87 039 423	1 415	411 072 799	0.8253
Scenario 7	67 990 349	3 927 064	1 866	10 303 888	82 223 167	1 415	415 797 513	0.8349
Scenario 8	66 832 589	3 927 460	1 869	10 351 900	81 113 818	1 415	416 980 800	0.8372

Table F.9: Yearly ReCiPe indicator points of the D6 processes.

	Heat	Electricity	Process water	Amine	Total RCP	CO2 captured	RCP/tCO2
Base case	20 536 629	412 800	131	2 573 171	23 522 731	1 414	46.7801
Layout 1	11 129 913	47 616	115	2 560 777	13 738 421	1 400	27.3491
Layout 2	12 787 200	415 872	136	2 582 826	15 786 034	1 416	31.0388
Scenario 1	20 449 118	412 416	137	2 572 840	23 434 512	1 415	46.6752
Scenario 2	20 673 141	412 416	131	2 571 100	23 656 787	1 415	47.1079
Scenario 3	20 590 810	395 904	131	2 574 213	23 561 058	1 415	46.9502
Scenario 4	36 864 000	450 816	121	2 553 559	39 868 496	1 415	80.7255
Scenario 5	14 696 085	395 520	238	2 486 836	17 578 679	1 415	35.2722
Scenario 6	21 350 610	412 416	131	2 571 475	24 334 632	1 415	48.3983
Scenario 7	19 412 158	416 256	131	2 595 494	22 424 039	1 415	44.6693
Scenario 8	20 917 055	415 872	131	2 422 563	23 755 621	1 415	47.2994

Table F.10: Yearly ReCiPe indicator points of the D9 processes

	Heat	Electricity	Process water	Amine	Total RCP	CO2 captured [kmol/hr]	RCP/tCO2
Base case	6 945 120	377 245	212	623 591	7 946 167	1 415	15.9539
Layout 1	5 821 540	15 464	207	629 942	6 467 153	1 413	13.001
Layout 2	6 336 000	400 199	211	641 805	7 378 215	1 444	14.5095
Scenario 1	7 008 862	374 118	214	627 216	8 010 411	1 423	15.9891
Scenario 2	6 908 950	377 490	212	625 282	7 911 934	1 415	15.8773
Scenario 3	6 915 463	377 614	212	625 450	7 918 739	1 416	15.8852
Scenario 4	6 029 706	398 117	200	645 885	7 073 908	1 416	14.1937
Scenario 5							
Scenario 6	7 281 168	392 807	213	624 855	8 299 042	1 415	16.661
Scenario 7	6 799 035	392 706	212	625 224	7 817 177	1 415	15.6965
Scenario 8	6 683 259	392 746	212	628 137	7 704 354	1 415	15.4677

G

Additional graphs and illustrations

G.1 Environmental assessment

Here the additional assessments of the environmental impact of the different will be seen. The graphs represent the effect of the sensitivity analyses on the different indicator results used to evaluate the environmental impact. The different sensitivity scenarios can be seen in section 4.7.2.

The sensitivity analyses for the cumulative energy demand indicator:

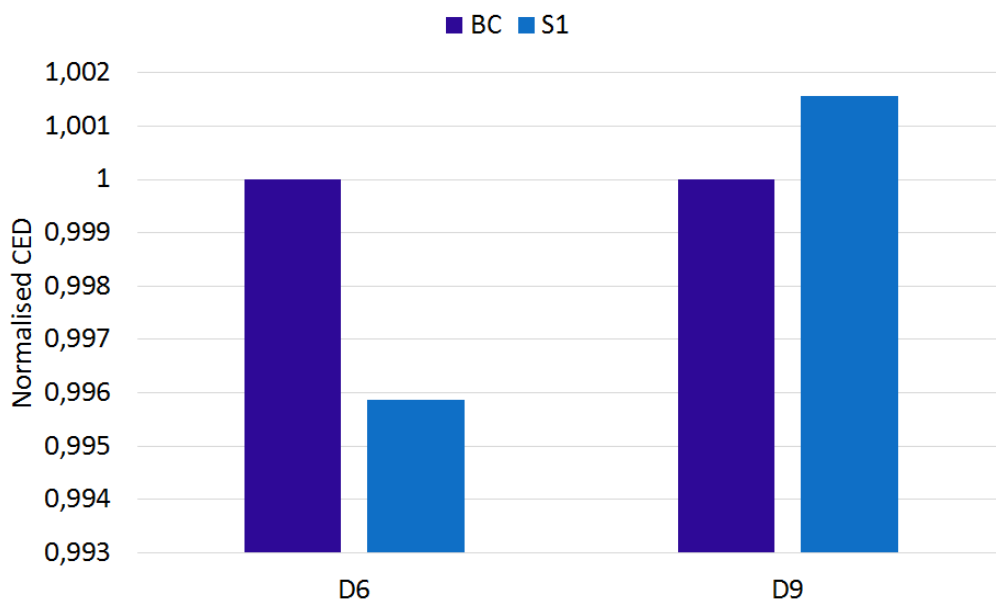


Figure G.1: Sensitivity analysis of the CED for scenario 1.

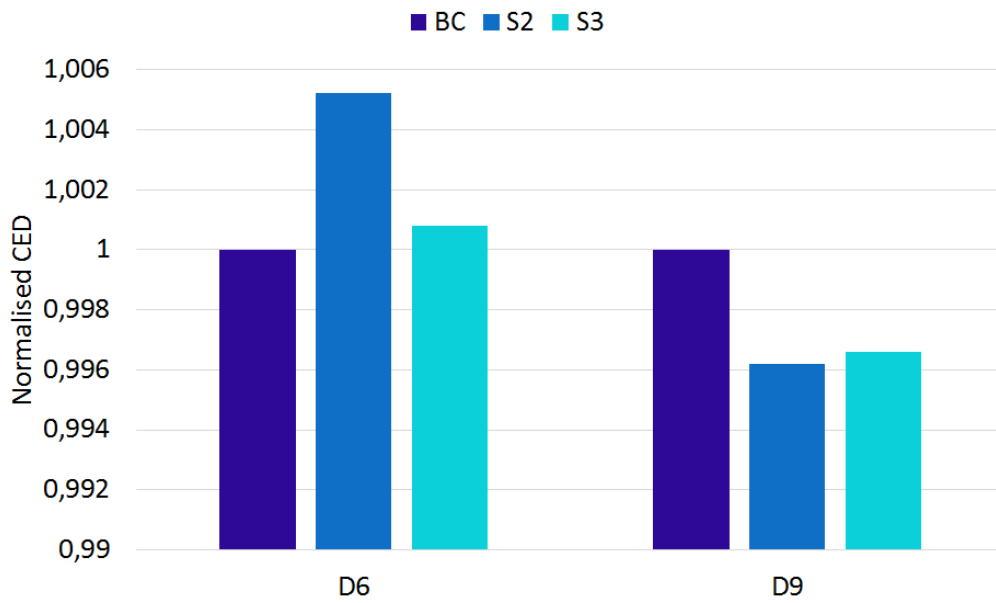


Figure G.2: Sensitivity analysis of the CED for scenarios 2 and 3.

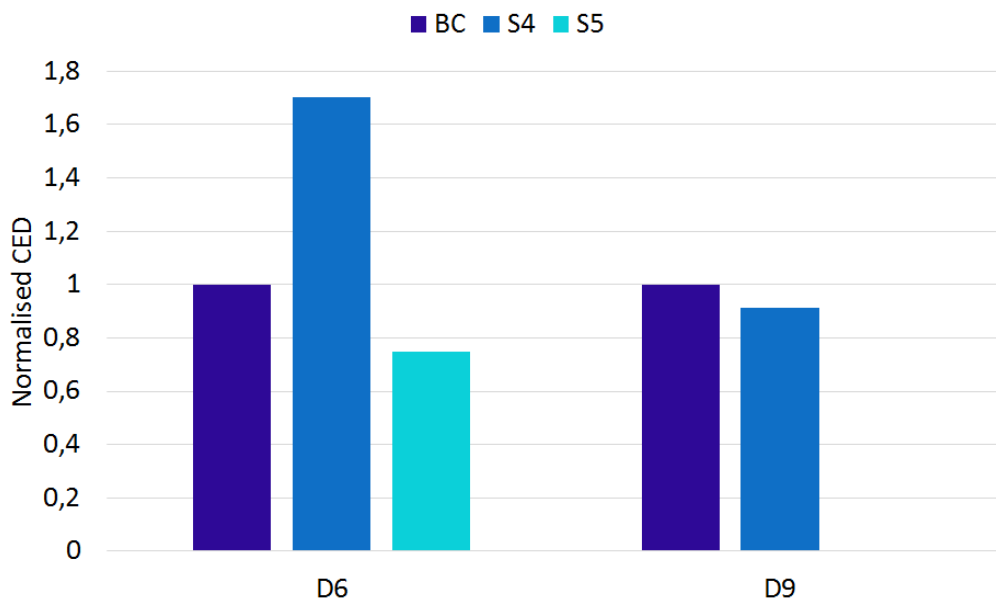


Figure G.3: Sensitivity analysis of the CED for scenarios 4 and 5.

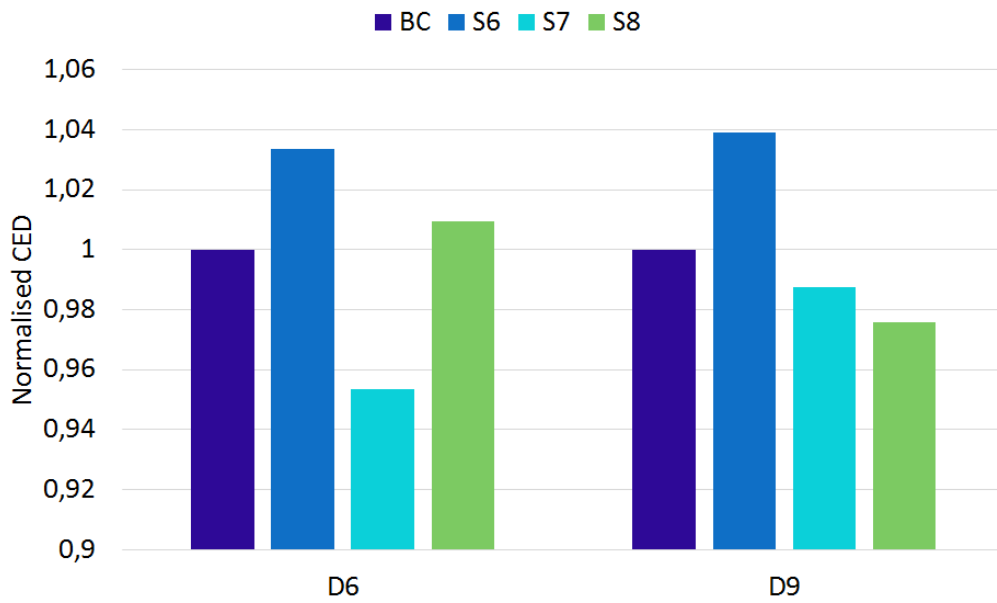


Figure G.4: Sensitivity analysis of the CED for scenarios 6, 7 and 8.

The sensitivity analyses for the global warming potential indicator:

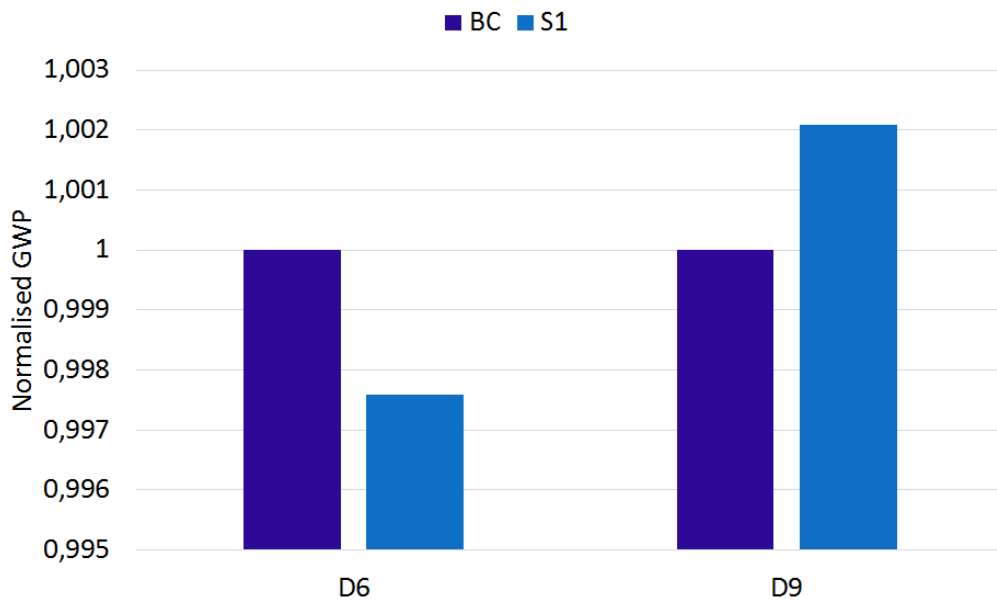


Figure G.5: Sensitivity analysis of the GWP for scenario 1.

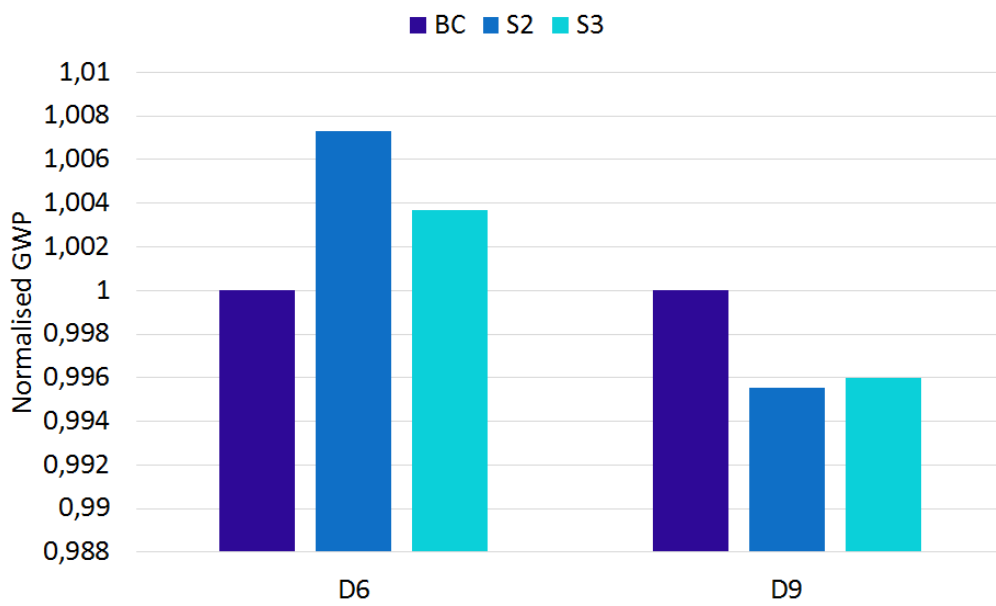


Figure G.6: Sensitivity analysis of the GWP for scenarios 2 and 3.

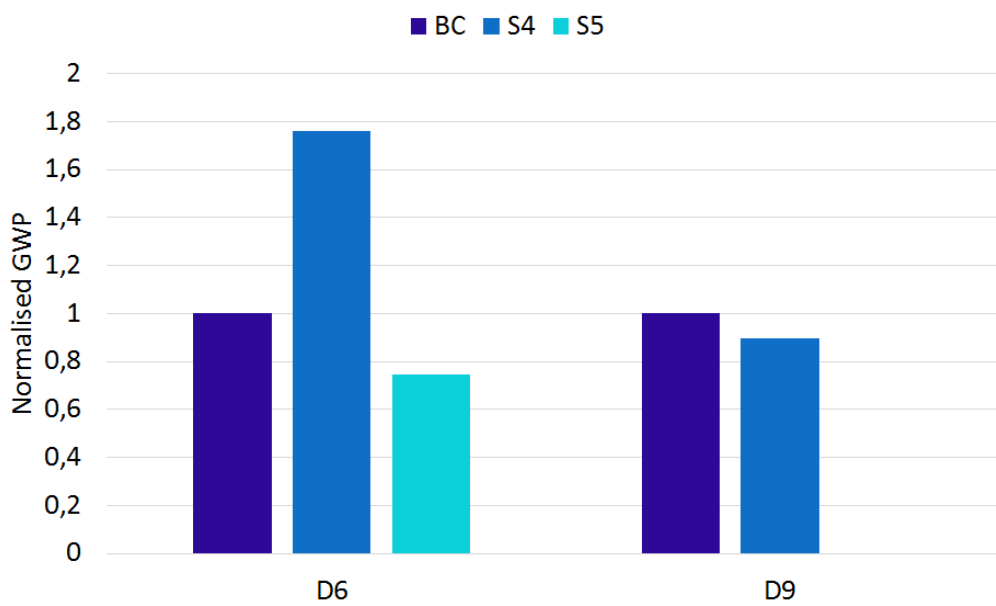


Figure G.7: Sensitivity analysis of the GWP for scenarios 4 and 5.

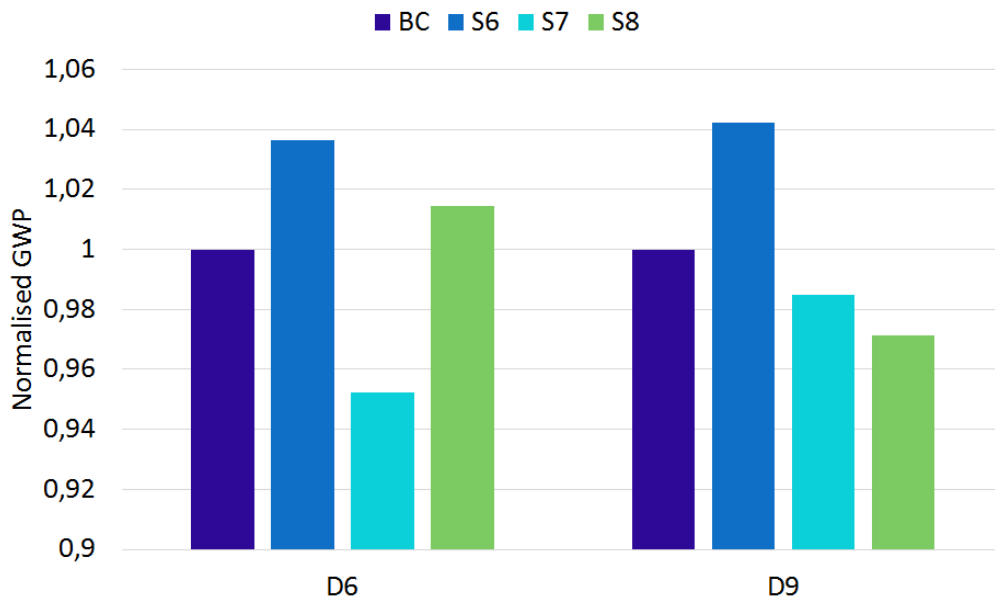


Figure G.8: Sensitivity analysis of the GWP for scenarios 6, 7 and 8.

The sensitivity analyses for the RCP indicator:

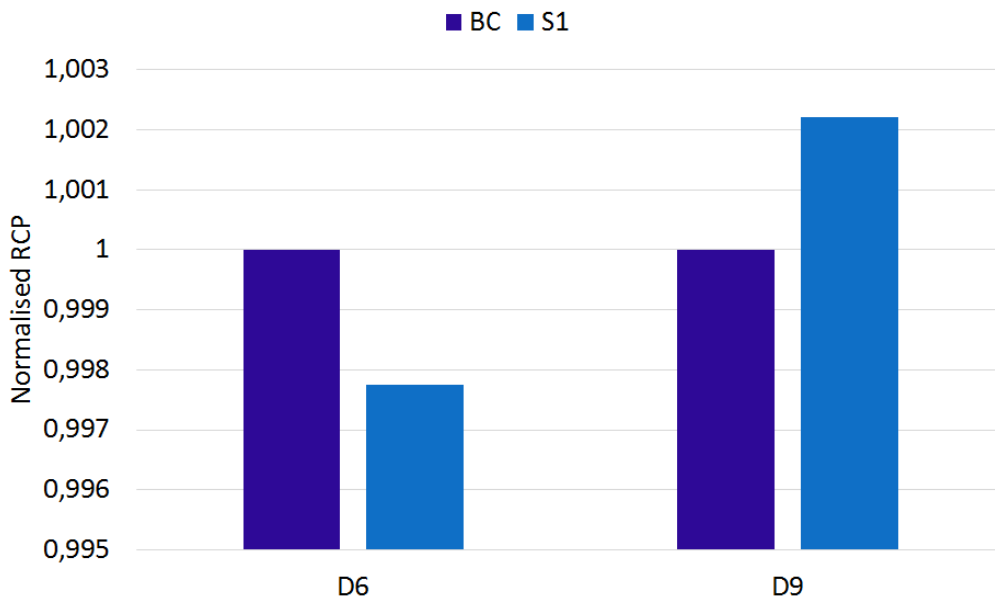


Figure G.9: Sensitivity analysis of the RCP for scenario 1.

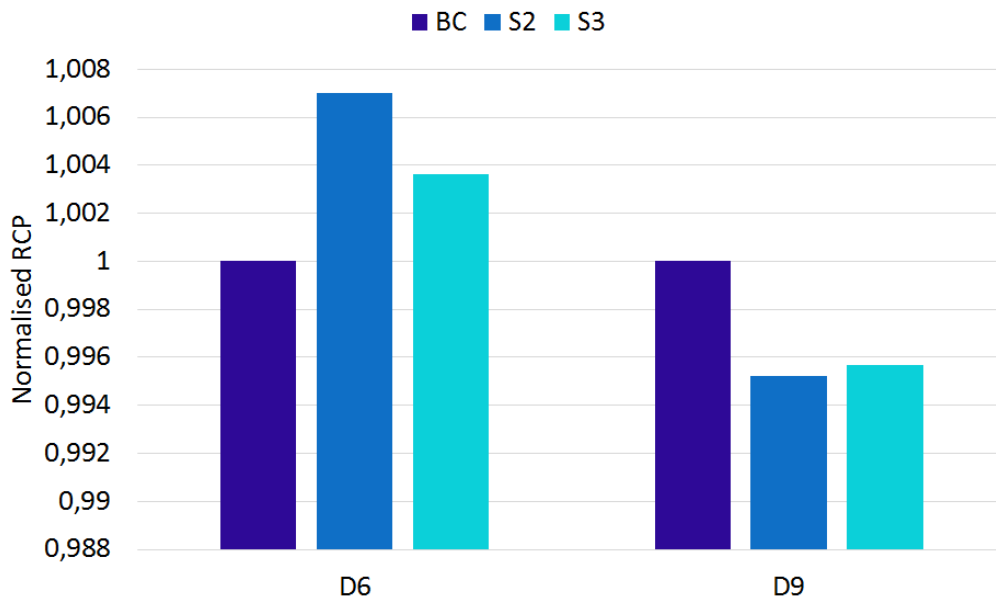


Figure G.10: Sensitivity analysis of the RCP for scenarios 2 and 3.

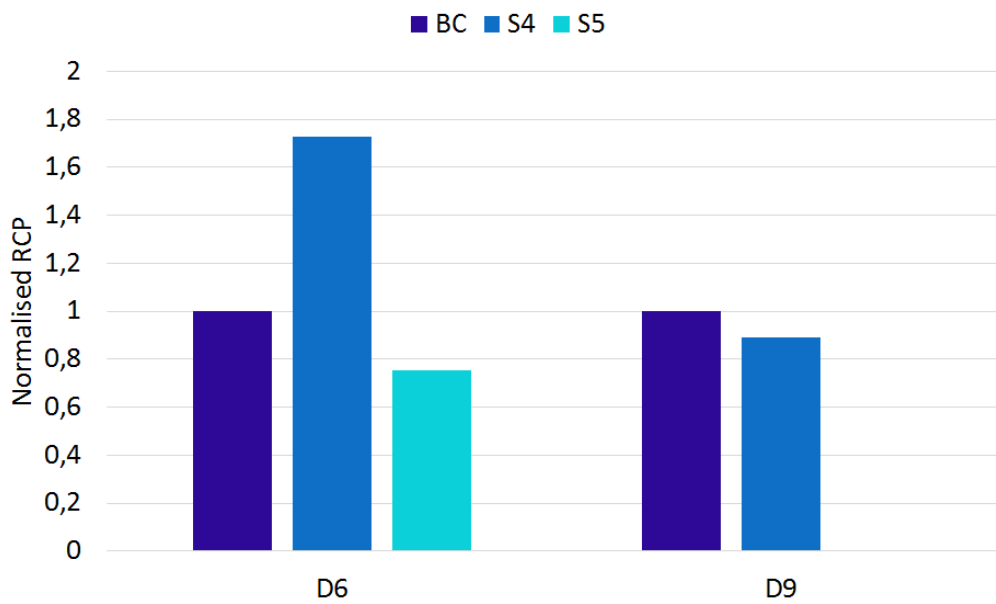


Figure G.11: Sensitivity analysis of the RCP for scenarios 4 and 5.

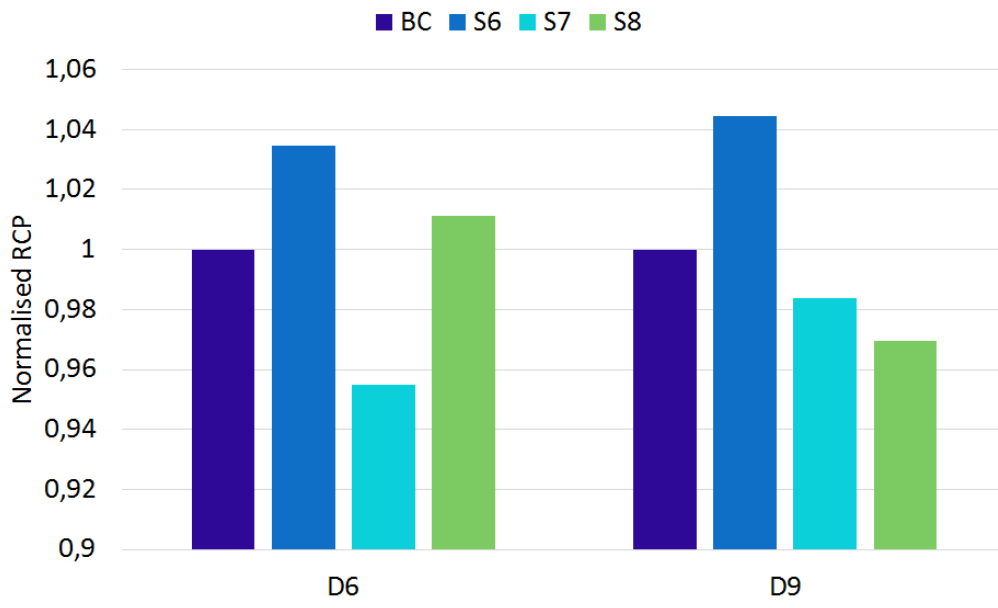


Figure G.12: Sensitivity analysis of the RCP for scenarios 6, 7 and 8.